https://doi.org/10.5194/egusphere-2025-778
Preprint. Discussion started: 26 February 2025
© Author(s) 2025. CC BY 4.0 License.

Seasonal isoprene emission estimates over tropical South America inferred from satellite observations of isoprene

Shihan Sun[1,2], Paul I. Palmer[1,2], Richard Siddans[3,4], Brian J. Kerridge[3,4], Lucy Ventress[3,4], Achim Edtbauer[5], Akima Ringsdorf[5], Eva Y. Pfannerstill[5], Jonathan Williams [5,6]

[1]National Centre for Earth Observation, University of Edinburgh, Edinburgh, EH9 3FF, UK
[2]School of GeoSciences, University of Edinburgh, Edinburgh, EH9 3FF, UK
[3]Remote Sensing Group, STFC Rutherford Appleton Laboratory, Chilton, Oxfordshire, OX11 0QX, UK
[4]National Centre for Earth Observation, STFC Rutherford Appleton Laboratory, Chilton, Oxfordshire, OX11 0QX, UK
[5]Max Planck Institute for Chemistry, Atmospheric chemistry department, Mainz, Germany
[6]Climate and Atmosphere Research Center (CARE-C), The Cyprus Institute, 1070 Nicosia, Cyprus

Correspondence to: Susie.Sun@ed.ac.uk

Abstract. Isoprene, a volatile organic compound (VOC) emitted by plants, plays a significant role in atmospheric chemistry and climate. The Amazon rainforest is a globally-relevant source of atmospheric isoprene, influencing regional and global atmospheric composition. We report isoprene emissions for 2019 inferred from a full-physics retrieval of isoprene columns from the Cross-track Infrared Sounder (CrIS) and the local sensitivities between isoprene emissions and isoprene columns determined by the GEOS-Chem chemical transport model. Compared with the MEGAN bottom-up inventory of isoprene emissions, the isoprene emission estimates inferred from CrIS have different spatial and seasonal distributions with generally lower emission rates but with higher emission rates over the north of Amazon basin and southeast of Brazil. The observed mean isoprene concentration at the Amazon Tall Tower Observatory (ATTO), March—December 2019, is 3.0 ± 2.2 ppbv, which is reproduced better by the GEOS-Chem model driven by isoprene emissions inferred from CrIS (2.8 ± 1.4 ppbv) than by the MEGAN inventory (4.1±1.3 ppbv). GEOS-Chem model formaldehyde (HCHO) columns, corresponding to isoprene emissions inferred from CrIS, are generally more consistent with TROPOMI data (normalized mean error, NME = 43%) than the HCHO columns corresponding to MEGAN isoprene emissions (NME = 50%), as expected. They also improve the model agreement with regional TROPOMI HCHO:NO_2 column ratios that are indicative of changes in photochemical regime. Our results provide confidence that we can use CrIS data to examine future impacts of anthropogenic activities, such as deforestation and land-use change, on isoprene emissions from the Amazon.

1 Introduction

Tropical South America, including the Amazon rainforest, hosts important ecosystems that influence the global carbon and water cycles. Amazonia is also a significant but uncertain source of biogenic volatile compounds (BVOCs), dominated by mass by isoprene (Guenther et al., 2006), that influences atmospheric chemical composition on local to global scales

https://doi.org/10.5194/egusphere-2025-778
Preprint. Discussion started: 26 February 2025
© Author(s) 2025. CC BY 4.0 License.

(Wiedinmyer et al., 2006; Yáñez-Serrano et al., 2015; Millet et al., 2016; Gomes Alves et al., 2023; Mayhew et al., 2023; Ringsdorf et al., 2023; Ferracci et al., 2024). Isoprene has an e-folding lifetime of ~1 hour against oxidation by hydroxyl radical (OH) and plays a role in ozone chemistry (Atkinson, 2000; Saunier et al., 2020), production of secondary organic aerosol (Claeys et al., 2004; Kroll et al., 2005, 2006; Carlton et al., 2009), and by modifying the levels of OH (Lelieveld et al., 2008; Hofzumahaus et al., 2009; Fuchs et al., 2013; Millet et al., 2016; Nölscher et al., 2016; Hansen et al., 2017; Pfannerstill et al., 2021). Isoprene also influences the lifetimes of other pollutants, e.g. carbon monoxide (Miyoshi et al., 1994) and methane (Feng et al., 2023). Evidence suggests that plants emit isoprene to protect leaf biochemistry under environmental stress (Sharkey et al., 2007; Monson et al., 2013; Zeinali et al., 2016), which is also seen as a key plant trait that determines species responses to rising temperature and drought (Taylor et al., 2018; Werner et al., 2021; Byron et al., 2022). Changes in isoprene emissions due to deforestation, rising levels of atmospheric CO_2, and climate change induced land use and land cover changes will also play an important role in controlling future changes in biogenic emissions and thereby atmospheric composition (Fini et al., 2017; Chen et al., 2018; Yáñez-Serrano et al., 2020; Sahu et al., 2023).

Emission estimates of isoprene are particularly uncertain over the tropics where ground-based measurements are sparse. Satellite observations of formaldehyde (HCHO) have for the last 20 years helped to supplement these ground-based observations (Abbot et al., 2003; Palmer et al., 2003; Shim et al., 2005; Wiedinmyer et al., 2005; Palmer et al., 2006, 2007; Barkley et al., 2008; Millet et al., 2008; Müller et al., 2008; Barkley et al., 2009; Stavrakou et al., 2009; Kaiser et al., 2018; Surl et al., 2018; Opacka et al., 2021; Feng et al., 2024; Opacka et al., 2024). Formaldehyde is a high yield product of isoprene oxidation by OH and because HCHO has a lifetime of typically only several hours, observed changes in HCHO can be linked to emissions of the parent hydrocarbon (Palmer et al., 2003). Irrespective of the sophistication of the inverse method that is used to translate observed changes in HCHO to isoprene emission estimates (Shim et al., 2005; Kaiser et al., 2018) some form of atmospheric chemistry model is needed, typically a global 3-D model that includes atmospheric transport, so we remain reliant on the assumed *a priori* emission inventories (e.g. Guenther et al, 2006), the chemical networks and their respective uncertainties. For example, there remain substantial uncertainties associated with the production of HCHO from isoprene oxidation at low nitrogen oxide levels, which are found over the tropics away from biomass burning and urban centres (Lelieveld et al., 2008). Interpreting HCHO in terms of BVOC emissions also requires careful attention to discard data influenced by biomass burning (Barkley et al., 2008; Gonzi et al., 2011). HCHO can also be produced from sources other than isoprene, such as alkanes, alkenes, and monoterpene, resulting in uncertainties in HCHO inferred isoprene emissions (Marvin et al., 2017; Surl et al., 2018). Development of isoprene retrievals (Fu et al., 2019; Palmer et al., 2022; Wells et al., 2020, 2022) using data collected by the Cross-track Infrared Sounder (CrIS) has resulted in a new and independent capability to determine isoprene emissions more directly.

In this study, we use a nested version of GEOS-Chem chemical transport model to investigate the consistency of isoprene emission estimates inferred from CrIS isoprene retrievals and the bottom-up MEGAN isoprene emission inventory over

https://doi.org/10.5194/egusphere-2025-778
Preprint. Discussion started: 26 February 2025
© Author(s) 2025. CC BY 4.0 License.

tropical South America during 2019, and compare the *a posteriori* isoprene concentrations with *in situ* measurements collected from the Amazon Tall Tower Observatory (ATTO), located in the pristine rainforest. Section 2 describes the nested GEOS-Chem model configuration we use to interpret the satellite and *in situ* tall tower data, including the MEGAN isoprene emissions model; the TROPOMI and CrIS satellite data and the tall tower data; and the methods we use to translate the column data into emission estimates. In Sect. 3, we report our results. We compare our satellite-based emission estimates for isoprene with the inventory estimates from the MEGAN model and evaluate our CrIS derived estimates against the *in situ* tall tower atmospheric isoprene measurements, and estimates for isoprene drivers, e.g. temperature, photosynthetic active radiation. We also compare observed HCHO:NO_2 ratios with model values driven by MEGAN and isoprene emissions inferred from CrIS satellite observations to examine whether the revised emission data could better describe the ozone production regimes across the region. We conclude our study in Sect. 4.

2 Data and Methods

Here we describe the GEOS-Chem atmospheric chemistry model that relates surface emissions of BVOCs, including isoprene, and atmospheric columns of isoprene and HCHO. We describe the satellite observations of isoprene from CrIS and HCHO from TROPOMI, and the tall tower measurements of atmospheric isoprene collected in central Amazonia that we use to evaluate the model. We also describe the methods that we use to translate these data into estimates of isoprene emission.

2.1 GEOS-Chem simulations

We use GEOS-Chem v14.1.0 atmospheric chemical transport model (https://geoschem.github.io, last access: 5 Dec 2024). GEOS-Chem is driven by Goddard Earth Observing System-forward processing (GEOS-FP) assimilated meteorological analyses from the NASA Global Modelling and Assimilation Office at NASA Goddard Earth Observing System. Nested model simulations are conducted at a horizontal resolution of 0.25° × 0.3125° using 47 vertical levels, of which 30-35 are within the troposphere, over a spatial domain centred over tropical South America: 35° S—15° N, 85°W—30° W. A buffer zone of 3° is applied along each of the four lateral boundaries of the nested domain. We generate lateral boundary conditions for the nested model using a self-consistent global model run at a horizontal resolution of 2° × 2.5°, following a one year spin-up from Jan 2018 through December 2019.

We use the complex secondary organic aerosol (SOA) and semi-volatile primary organic aerosol (SVPOA) mechanism, which includes the full-chemistry "tropchem" mechanism to describe gas-phase reactions (Eastham et al., 2014) and the photochemical production of SOA and SVPOA with up-to-date isoprene mechanisms (Bates and Jacob, 2019). The "complex–SOA_SVPOA" mechanism uses a combination of explicit aqueous uptake mechanisms (Marais et al., 2016) with a standard volatility basis set scheme (Pye et al., 2010).

https://doi.org/10.5194/egusphere-2025-778
Preprint. Discussion started: 26 February 2025
© Author(s) 2025. CC BY 4.0 License.

We use the standard Harvard-NASA Emissions Component (HEMCO) configuration, including biogenic emissions from the Model of Emissions of Gases and Aerosols from Nature (MEGAN v2.1) inventory (Guenther et al., 2012). To test the isoprene emissions inferred from the satellite data, we use offline BVOC emissions at 0.25° × 0.3125° horizontal resolution which are pre-computed using MEGAN v2.1 and modify the emission rates. Pyrogenic emissions are from the Global Fire Emissions Database version 4.1 that includes small fire correction (Van Der Werf et al., 2017). The GFED inventory provides monthly dry matter emissions based on satellite observations of fire activity and vegetation coverage from MODIS. Anthropogenic emissions, including fossil and biofuel sources, are from the Community Emissions Data System inventory (CEDS v2), which provides CMIP6 historical anthropogenic emissions data from 1750 to 2019 mapped to a 0.5° global grid (Hoesly et al., 2018).

MEGAN has been extensively used to calculate isoprene emission rates in climate models (Guenther et al., 2006, 2012). The algorithm of isoprene emission rates in MEGAN v2.1 is based on plant functional type (PFT) specific emission rates adjusted by empirical scaling functions dependent on environmental and meteorological variables. Large uncertainties remain for the base isoprene emission rates (Arneth et al., 2008) and for the empirical parameterizations of plant responses to temperature and drought (Jiang et al., 2018; Seco et al., 2022; Bourtsoukidis et al., 2024). Studies have reported significant discrepancies between MEGAN and isoprene emission estimates and atmospheric isoprene data from satellite and in-situ observations, especially for tropical forests (Warneke et al., 2010; Bauwens et al., 2016; Wang et al., 2017; Gomes Alves et al., 2023). Some studies found MEGAN v2.1 overestimated isoprene emissions over the tropics compared with emission estimates inferred from satellite observations of HCHO (Marais et al., 2012; Barkley et al., 2013; Stavrakou et al., 2014; Worden et al., 2019), while other studies using ground based or aircraft measurements found the opposite (Gu et al., 2017). Gaps also remain in the parameterization of PFT-specific responses under severe climates. Droughts and heat waves have been found to impact isoprene emissions (Seco et al., 2015; Ferracci et al., 2020), yet current models struggle to capture plant responses under climate extremes (Huang et al., 2015; DiMaria et al., 2023). Despite that satellite-based land cover products are used to constrain isoprene emission calculations, uncertainties remain in these remotely sensed vegetation maps due to their coarse resolution and the mapping of PFTs (Opacka et al., 2021). The remarkable species composition in tropical forests makes it difficult to link emission factors and functional relationships to individual PFTs.

To compare model simulations with satellite retrievals, GEOS-Chem simulated profiles are sampled at the satellite overpassing time and location of each measurement for both TROPOMI and CrIS. We then interpolate model profiles to the vertical levels of satellite retrievals. For consistency between satellite and GEOS-Chem simulated vertical profiles, we also apply scene-dependent averaging kernels that describe the instrument vertical sensitivity to changes in a trace gas and replace any *a priori* information assumed by the retrieval and then integrate from the surface up to the tropopause to calculate column values.

https://doi.org/10.5194/egusphere-2025-778
Preprint. Discussion started: 26 February 2025
© Author(s) 2025. CC BY 4.0 License.

2.2 CrIS isoprene retrievals

We use CrIS isoprene column average retrievals from RAL's Infrared and Microwave Sounding (IMS) scheme (Palmer et al., 2022). CrIS is a Fourier transform spectrometer covering three IR spectral regions spanning 650–2550 cm^{-1} onboard the Suomi-National Polar-orbiting Partnership (S-NPP) satellite in October 2011 and NOAA-20 in November 2017 into sun-synchronous low Earth orbits with overpass times of 01:30 and 13:30 local time. CrIS has comparatively low noise in the spectral region in which isoprene features occur which, together with more favourable thermal structure at ~13:30 than 9:30 make detection of isoprene feasible for CrIS. Other than instrumental noise, uncertainty in CrIS retrieved isoprene column averages principally concerns the adopted vertical profile shape, which is a constant volume mixing ratio, and CrIS vertical sensitivity, which is accounted for explicitly in the analysis by applying vertical averaging kernels to the model profiles. Although the *a priori* constraint on the retrieval is weak, this is also accounted for. As in Palmer et al (2022), CrIS isoprene data are filtered to exclude scenes with extensive thick or high cloud and retrievals with a high cost function (i.e., poor spectral fit). Due to the simple, adopted profile shape and decrease in sensitivity near surface level in absence of significant surface-air temperature contrast, IMS column averages tend to be lower than those derived from surface-based observations where surface level concentrations are high. In this study, we use daytime satellite retrieved isoprene columns which correspond with peak isoprene emissions.

2.3 TROPOMI column retrievals of HCHO and NO_2

TROPOMI was launched onboard of the Copernicus Sentinel-5 Precursor (S5P) satellite on 13 October 2017 into a low-Earth polar orbit with am equatorial local overpass time of 13:30 (Veefkind et al., 2012). TROPOMI is a nadir viewing instrument that collected data at ultraviolet, visible, near infrared, and shortwave infrared wavelengths. TROPOMI has a horizontal swath of 2600 km that is divided into 450 across-track rows. The spatial resolution of TROPOMI at nadir is 3.5×7 km^2 (across-track × along-track) which was later refined to 3.5×5.5 km^2 in August 2019 due to an adjustment to the along track integration time. TROPOMI NO_2 retrievals use wavelengths from 400 to 496 nm and HCHO retrievals using wavelengths from 320 to 405nm. We refer to the reader to dedicated reported on these retrieved data products for further details (De Smedt et al., 2018; Van Geffen et al., 2022). We use the operational offline TROPOMI level 2 quality control retrievals for HCHO and NO_2 columns. To remove retrievals with substantial errors or those influenced by clouds or snow/ice cover we use the retrieval quality assurance (QA) flag provided by the data products. We discard data with QA flags > 0.75 for NO_2 and > 0.5 for HCHO, following recommendations (De Smedt et al., 2020; Eskes and Eichmann, 2022)

TROPOMI has a better signal-to-noise ratio compared to Ozone Monitoring Instrument (OMI) but the HCHO observations still have a bias against ground-based multi-axis differential optical absorption spectroscopy instruments (De Smedt et al., 2021). TROPOMI retrievals of HCHO were found to underestimate high columns and overestimate low columns in previous studies (Vigouroux et al., 2020; Müller et al., 2024). Noting that biases for OMI and TROPOMI HCHO columns are

https://doi.org/10.5194/egusphere-2025-778
Preprint. Discussion started: 26 February 2025
© Author(s) 2025. CC BY 4.0 License.

expected to be similar (De Smedt et al., 2021), we have applied a bias-correction formula recently proposed for HCHO columns from OMI (Müller et al., 2024): $\Omega_{HCHO,BC} = (\Omega_{HCHO} - 2.5x10^{15})/0.655$, where $\Omega_{HCHO,BC}$ denotes the bias-corrected HCHO columns (molec cm^{-2}). We find that applying this bias does not change the conclusions of our paper.

2.4 Amazon Tall Tower Observatory (ATTO)

We use data collected at the Amazon Tall Tower Observatory (ATTO, 2º8'S, 59º0'W) site located in central Amazonia (Gomes Alves et al., 2023) to independently evaluate the GEOS-Chem model. The characteristics of this site have been described extensively in Andreae et al. (2015). The anthropogenic influence from the closest city Manaus (150 km southwest of ATTO) is negligible and the site has been established to represent pristine tropical forest conditions throughout the year. The tropical climate at this broader geographical region includes a dry season (July – October) and a wet season (December – May) associated with seasonal rainfall amounts of less than 100 mm and over 200 mm, respectively (Botía et al., 2022). We use air measurements that were collected at 80m, 150m and 320m respectively from March to December 2019. The measurements were made using a Proton Transfer Reaction Time of Flight Mass Spectrometer (PTR-ToF-MS Ionicon Austria) as described by Ringsdorf et al. 2023. For the purposes of comparison with the model, we calculate the mean hourly observed isoprene concentrations from these three levels.

2.5 Method to infer satellite-derived isoprene emission inventory

We use CrIS retrievals of isoprene column (Ω_{isop}), described above, to derive the isoprene emission rates that we use within the GEOS-Chem model. To understand the relationships these isoprene columns to isoprene emissions, we regress MEGAN isoprene emission rates $E_{isop,GC}$ (kg m^{-2} s^{-1}) with GEOS-Chem model Ω_{isop}, sampled at the CrIS local overpass time of 13:30 within each grid box for each month, and keep the grid boxes where the linear regression model can explain a significant amount of variance in isoprene emission rates (p-value < 0.05). To determine monthly isoprene emission rates from satellite retrievals from CrIS, we rearrange the regression model and insert the observed columns: $E_{isop,sat} = (\Omega_{sat} - B)/S$, where $E_{isop,sat}$ is the isoprene emission estimate inferred by satellite data, Ω_{sat} refers to the CrIS column data, and S is mainly determined by isoprene lifetime. We use a similar approach to relate TROPOMI HCHO columns (Ω_{HCHO}) to isoprene emission estimates. For the analysis of HCHO data, the S in the regression model is determined by the HCHO yield from isoprene oxidation and by the HCHO lifetime.

Given the lifetime of isoprene against oxidation by OH and the mean wind speed we estimate that most of the isoprene lost and the associated HCHO production is on a scale shorter than a 2º × 2.5º grid box but typically longer than an individual 0.25º × 0.3125º grid box. Consequently, to remove this potential "smearing effect" on the finer horizontal resolution, we calculate our linear regression relationships using a horizontal resolution of 2º × 2.5º, following recent studies (Wells et al., 2020, 2022).

https://doi.org/10.5194/egusphere-2025-778
Preprint. Discussion started: 26 February 2025
© Author(s) 2025. CC BY 4.0 License.

To implement this regression approach, we first compute the linear regression relationships within each grid for each month using daily MEGAN isoprene emission estimates and the corresponding model values for Ω_{HCHO} and Ω_{isop} sampled at the equatorial overpass time of the satellite, 2018—2020, inclusively. We then use these grid-based regressions models to infer monthly isoprene emission estimates for 2019. For model grid boxes for which emission rates cannot be estimated, e.g., p-value > 0.05 or missing data, we use data from the immediately adjacent grids (nearest neighbours) to recalculate the regression models, as described above. We then relate the monthly $E_{isop,sat}$ values, representative of the 13:30 local overpass time of CrIS and TROPOMI, to the diurnal variation in isoprene emission rates by using scaling factors derived from diurnal and day-to-day variations in the offline MEGAN isoprene emission rates for 2019. The magnitude of satellite inferred isoprene emission rates for 2019 is scaled by the ratio of monthly MEGAN emission rates in 2019 relative to the 2018-2020 monthly mean. The default isoprene emission rates are then replaced with CrIS derived isoprene rates and regridded to the nested 0.25° × 0.3125° GEOS-Chem model resolution.

To remove the influence of biomass burning on the HCHO regressions models, we discard data for which there are fire counts identified by the NASA Fire Information for Resource Management System (FIRMS) active daily fire data acquired by the MODerate-resolution Imaging Spectroradiometer (MODIS) sensors (https://firms.modaps.eosdis.nasa.gov/, last access: 15 Nov, 2024). These fire counts are determined by thermal IR anomalies by the MODIS sensors aboard Aqua and Terra satellites at a 1km horizontal resolution. We select daytime fire counts with a high confidence level, i.e., higher than or equal to 80% as recommended in the MODIS user's guide (Giglio et al., 2020).

3 Results and discussion

We report the isoprene emission estimates inferred from CrIS isoprene and TROPOMI HCHO column data during 2019, which we evaluate using *in situ* data collected at ATTO.

3.1 CrIS inferred isoprene emissions

Figure 1 compares monthly mean CrIS and GEOS-Chem (MEGAN) isoprene columns for year 2019. Both GEOS-Chem and CrIS show a strong seasonal cycle, with a peak monthly mean Ω_{isop} in August. GEOS-Chem (MEGAN) and CrIS report the lowest monthly Ω_{isop} in April and November, respectively. The best agreement between GEOS-Chem (MEGAN) and CrIS for 2019 is found mainly during dry months, from June to August, with Pearson correlation coefficients R=0.59—0.73, p < 0.05, and with normalized mean biases (NMB) of 20% to 38%. The largest discrepancies between GEOS-Chem and CrIS typically occur during relatively wet months (regional mean total precipitation > 5mm day^{-1}). GEOS-Chem (MEGAN) has a positive bias with respect to CrIS (NMB > 100%) over the Amazon Basin throughout the year with the highest positive biases over the western Amazon basin as shown in Fig.1. Despite the overall positive biases, the model underestimates Ω_{isop}

https://doi.org/10.5194/egusphere-2025-778
Preprint. Discussion started: 26 February 2025
© Author(s) 2025. CC BY 4.0 License.

over southeast Brazil where it is dominated by savanna, with the largest negative biases during the dry season. These seasonal and regional model biases have also been found in previous studies (e.g., Wells et al., 2020). Hotspots of Ω_{isop} during the wet season are mainly observed to the north of the Amazon basin, on the borders between Columbia, Venezuela, and Brazil, where the land cover is dominated by tropical rainforest. In contrast, GEOS-Chem (MEGAN) shows regional hotspots along the east of the Andes, over western Brazil, and eastern Peru. Elevated values of CrIS Ω_{isop} over northern Amazonia has been independently observed by aircraft measurements (Gu et al., 2017), suggesting possible negative model bias where the tropical plant species distributions may not be well represented by the model.

Previous studies have reported significant spatial differences between bottom-up emission inventories of isoprene and satellite column observations of isoprene (Fu et al., 2019; Wells et al., 2022; J.-F. Müller et al., 2024). To understand these differences, we calculate top-down values of E_{isop} using satellite column retrievals of isoprene and HCHO to compare with the MEGAN bottom-up inventory for E_{isop}. The isoprene chemistry in the current version of GEOS-Chem appears to be able to reproduce HCHO at low NOx levels over the Amazonian region (Bates and Jacob, 2019; Fu et al., 2019; Wells et al., 2020). We use the relationships between isoprene emissions and isoprene columns described in GEOS-Chem to derive E_{isop} from CrIS Ω_{isop}, and we also calculate E_{isop} derived from TROPOMI Ω_{HCHO} to compare with CrIS derived E_{isop}. For those model grids where the $E_{isop} \sim \Omega_{sat}$ linear relationships are not significant (p-value > 0.05), or satellite inferred isoprene emissions are negative, we assume no isoprene emissions within these grids which may cause an underestimation of E_{isop} in some areas. Figure 1 also shows the monthly location of fires identified by MODIS data. It clearly shows that for large parts of the Amazon, isoprene emission estimates inferred from HCHO are compromised by fire (Barkley et al., 2008, 2011) and for these locations we remove days with fire incidents when computing $E_{isop} \sim \Omega_{sat}$ linear relationships.

https://doi.org/10.5194/egusphere-2025-778
Preprint. Discussion started: 26 February 2025
© Author(s) 2025. CC BY 4.0 License.

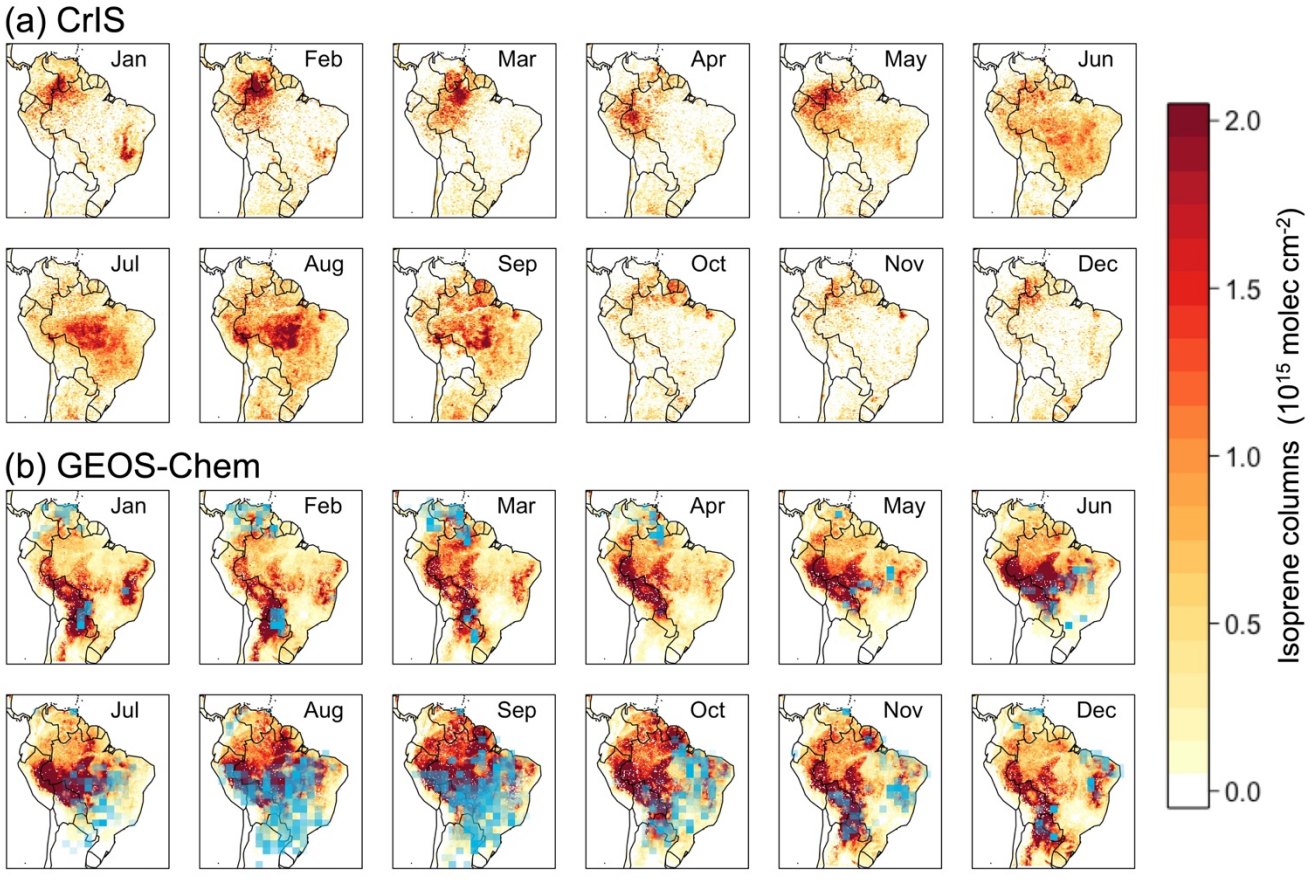

Figure 1: Monthly mean (a) CrIS and (b) GEOS-Chem isoprene columns (10^{15} molec cm^{-2}) driven by MEGAN emissions sampled at the CrIS local overpass time of 13:30 for 2019. GEOS-Chem model columns include scene-dependent CrIS averaging kernels. Blue boxes in (b) indicate fire intensities and locations from MODIS.

Figure 2a shows monthly total isoprene emission estimates from MEGAN and with estimates inferred from CrIS isoprene and TROPOMI HCHO column data over the spatial domain showed in Fig. 1 where monthly isoprene emission rates can be inferred from both CrIS and TROPOMI data. TROPOMI and CrIS inferred isoprene emission estimates peak in September, while MEGAN peaks during October to December. TROPOMI derived isoprene emission estimates are 17~63% lower than MEGAN, except during peak fire months of August and September. CrIS is also lower than MEGAN, but with a smaller discrepancy than for TROPOMI, except for May—September. We remove Ω_{HCHO} values that coincide with MODIS detected fires, resulting in lower TROPOMI Ω_{HCHO} derived isoprene emissions during the months where isoprene hotspots collocated with fire incidents as shown in Fig. 1. Recent work also found that OMI HCHO based isoprene emissions were significantly lower than the CrIS-derived emissions (from a different CrIS retrieval scheme) over South America, with the largest discrepancies over Brazil (Müller et al, 2024). Figure 2b shows the spatial distribution of monthly mean isoprene emission

https://doi.org/10.5194/egusphere-2025-778
Preprint. Discussion started: 26 February 2025
© Author(s) 2025. CC BY 4.0 License.

rates for year 2019, inferred from the IMS CrIS isoprene column data. The corresponding monthly isoprene emission estimates from MEGAN and inferred from TROPOMI HCHO columns are shown in Fig. S1.

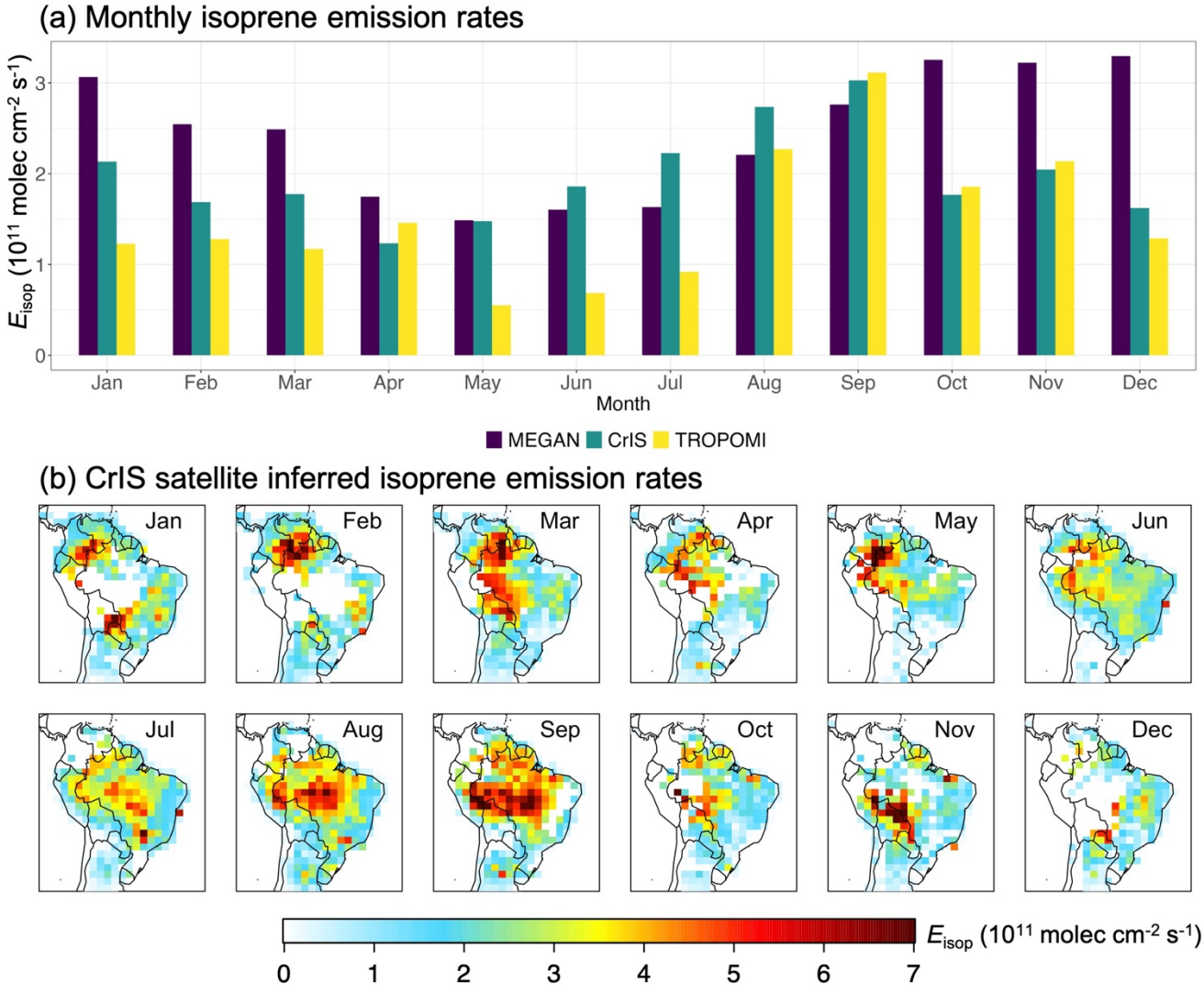

Figure 2: (a) Monthly mean MEGAN and satellite derived isoprene emission rates (10^{11} molec cm^{-2} s^{-1}) from MEGAN and as derived from CrIS isoprene and TROPOMI HCHO observations across tropical South America for 2019. (b) Monthly changes in the spatial distribution of the CrIS derived isoprene emission rates over tropical South America for 2019.

3.2 Model evaluation at ATTO

We conducted nested model simulations at a horizontal resolution of 0.25° × 0.3125°, driven by MEGAN and our CrIS derived isoprene emission estimates and compared the resulting hourly isoprene mixing ratios sampled at nearest grid boxes (Fig. 3a) to the ATTO tower. We acknowledge that the CrIS E_{isop} inferred at a horizontal resolution of 2° × 2.5° (Fig. 1), as

https://doi.org/10.5194/egusphere-2025-778
Preprint. Discussion started: 26 February 2025
© Author(s) 2025. CC BY 4.0 License.

described above, can only represent the mean isoprene emissions over that area. Figure 3a shows annual mean values for the enhanced vegetation index (EVI) from the MODIS instrument, which provide information about the greenness of vegetation. The highest values of EVI over the Amazon Basin are associated with tropical rainforests that have a comparatively small seasonal variation. Measurements collected at ATTO site should by design be representative of the surrounding rainforest within Amazon basin. As such, we assume that model isoprene mixing ratios over grid cells adjacent to ATTO, dominated by upland tropical rainforest with similar biome types, are comparable to the monthly isoprene concentrations observed at ATTO.

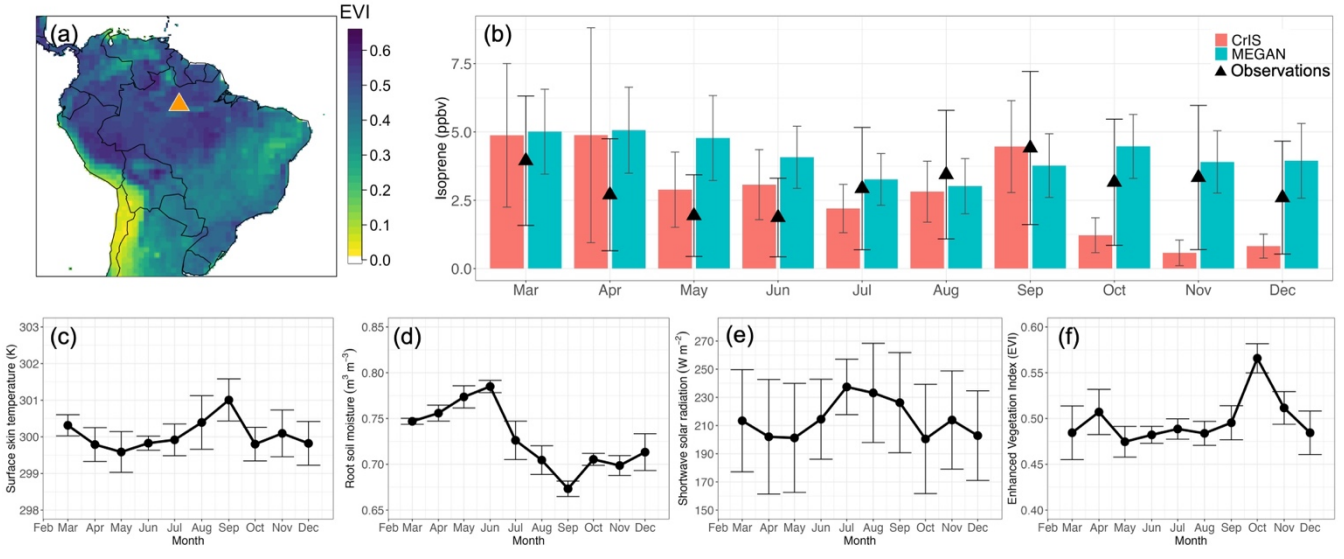

Figure 3: (a) Annual mean values of enhanced vegetation index (EVI) from MODIS. The ATTO site is marked by an orange triangle. (b) Model and observed monthly mean isoprene mixing ratios (ppbv) at ATTO site during March-December 2019. Model values are driven by MEGAN and by values determined by the CrIS satellite data. Vertical lines denote the standard deviations of the monthly means. Monthly mean values for (c) surface skin temperature, (d) root soil moisture, (e) shortwave solar radiation, and (f) EVI.

Figure 3b shows the comparison of observed monthly mean isoprene mixing ratios at ATTO and the GEOS-Chem model during March to December 2019. GEOS-Chem (MEGAN) reproduces the monthly mean ATTO data, with an annual mean isoprene mole fraction of 4.1 ± 1.3 ppbv compared with the observed annual mean value of 3.0 ± 2.2 ppbv. June and November are transitioning months between dry (December-May) and wet season (July-October). Here we classify June as wet month and November as dry month based on the root soil moisture (Fig. 3d). The model (MEGAN) overestimates ATTO data by 77% during the wet months (March-June, December), 4.6 ± 1.4 ppbv versus 2.6 ± 1.9 ppbv, but is much closer during the dry months (July-November), 3.7 ± 1.1 ppbv versus 3.5 ± 2.5 ppbv. Isoprene emission estimates inferred from CrIS result in an annual mean of 2.8 ± 1.4 ppbv, and 2.3 ± 1.0 ppbv and 3.3 ± 1.9 ppbv during the dry (July-November) and wet (March-June, December) months, respectively. The top-down isoprene emissions underestimate the observed values

https://doi.org/10.5194/egusphere-2025-778
Preprint. Discussion started: 26 February 2025
© Author(s) 2025. CC BY 4.0 License.

from October to December partly because low satellite observed isoprene columns as shown in Fig. 2b and because some of the grid boxes near the observational tower are set to zero emission rates where the regression relationship is not significant (p-value > 0.05), which may lower the mean simulated isoprene mole fractions at ATTO. Despite the discrepancies between model and site observations, isoprene emission estimates using CrIS isoprene retrievals can generally reproduce the magnitudes of isoprene mole fractions for most months and can better capture months with peak isoprene concentrations (March and September) compared with model using MEGAN.

Some previous studies have reported that MEGAN underestimates observed isoprene mole fractions due to uncertainties in landcover or to its temperature response parameterization (Gu et al., 2017; DiMaria et al., 2023), while others report that it overestimates measurements because of overestimated emission factors (Sarkar et al., 2020; Gomes Alves et al., 2023). Current emission models using a single-point approach to parameterize bottom-up relationships between vegetation species and isoprene emission rates, depending on the prescribed emission factors, that have large uncertainties due to the lack of heterogeneity in flux measurements collected over different spatial scales (Misztal et al., 2016; Batista et al., 2019). Consequently, uncertainties in the emission model parameterizations and time-dependent inputs to the model (e.g., landcover) can greatly compromise the model capability to capture isoprene variations over tropical rainforests. Uncertainties from leaf-level phenological traits such as leaf age or ecosystem-level plant biodiversity which also influence isoprene emissions are also difficult to measure, with very few observational sites, but can be partially addressed with satellite-based observations of optical wavelengths.

Figure 3c, 3d and 3e show monthly mean surface skin temperature, average root soil wetness, and shortwave solar radiation obtained from GEOS-FP during 2019, averaged over a broad geographical region that includes ATTO (Fig. 3a). Figure 3f shows EVI from MODIS. The monthly temperature peaks during September when soil wetness drops to a seasonal low. Seasonal values of shortwave radiation at the surface peak during July-September reflect a seasonal minimum in cloud coverage. The GEOS-Chem model driven by CrIS derived isoprene emissions and the ATTO isoprene data follow the broad seasonal cycle of surface temperature and shortwave radiation, as expected, but neither correlates with EVI. The GEOS-Chem model calculation, driven by MEGAN isoprene emission estimates, show higher values over April to June compared with observations that are close to the peak of soil moisture but before the peak values of shortwave radiation and temperature. The seasonality of isoprene emission is correlated with temperature variation due to the strong dependence of enzyme isoprene synthase on temperature (Monson et al., 1992). During dry months less cloud cover and stronger solar radiation can also enhance isoprene emissions (Kesselmeier and Staudt, 1999). Previous studies have shown that isoprene emission increases with temperature and moderate droughts, but severe drought can decrease isoprene emission (Werner et al., 2021; Byron et al., 2022). Seasonal discrepancies between model and observed isoprene concentrations may be due an incorrect model representation of soil water profiles that overestimates soil water storage during both seasons, resulting in higher isoprene emissions (Schmitt et al., 2023).

https://doi.org/10.5194/egusphere-2025-778
Preprint. Discussion started: 26 February 2025
© Author(s) 2025. CC BY 4.0 License.

3.3 Comparison of MEGAN and CrIS inferred isoprene emissions

325 We evaluate the CrIS inferred isoprene emission rates using TROPOMI Ω_{HCHO}. GEOS-Chem simulated Ω_{HCHO} depends largely on isoprene emissions over the studied region. So that any reduced biases in model HCHO can be attributed to the CrIS isoprene emission estimates. We further compare model HCHO:NO_2 ratios with satellite-based values to evaluate how well GEOS-Chem with the revised isoprene emission estimate can describe the regional ozone sensitivity.

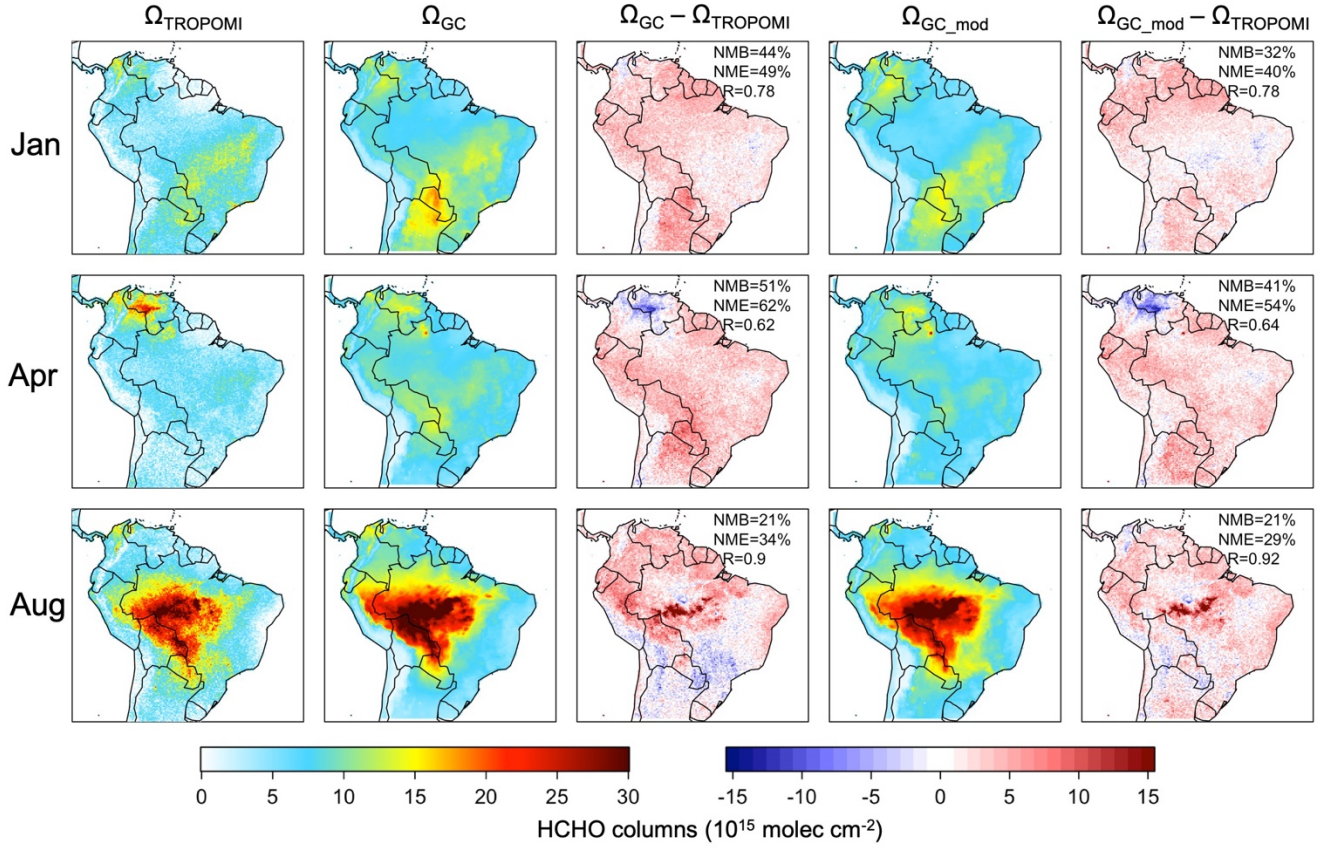

330 **Figure 4: TROPOMI (first column) and GEOS-Chem monthly mean HCHO columns (10^{15} molec cm^{-2}) for Jan, April, and Aug in 2019. The GEOS-Chem model columns driven by MEGAN (second column) and by CrIS derived isoprene emission estimates (fourth column). Difference between TROPOMI and model values are shown in third and fifth columns. Shown inset of panels in the third and fifth columns are the normalized mean biases (NMB), normalized mean error (NME), and the Pearson correlation coefficients (R).**

335 Figure 4 shows a monthly comparison between TROPOMI HCHO columns and GEOS-Chem driven by MEGAN and satellite-based CrIS derived isoprene emissions. The model generally captures the spatial distribution of monthly HCHO columns (R = 0.61 – 0.92). The model has a positive bias over most forested regions throughout the year, with a negative bias found over the tropical grasslands at the Colombia-Venezuelan plains to the north of the Amazon basin during March

https://doi.org/10.5194/egusphere-2025-778
Preprint. Discussion started: 26 February 2025
© Author(s) 2025. CC BY 4.0 License.

and April, as well as over the cropland to the southeast of the basin during the dry season. The CrIS derived isoprene emission inventory reduces the annual normalised mean error (NME) from 50% to 43% and reduces the NME from 58% to 47% during the wet season (December – May) and from 36% to 33% for the dry season (July – October). Over the Amazonian region (50~75ºW, 15ºS~ 5ºN), NME is reduced from 54% to 45% annually, and from 37% to 31 during dry season, from 65% to 53% during wet season. We report monthly statistics in Table S1.

Photochemical formation of ozone through nonlinear reactions involving sunlight, NOx, VOCs, and free radical species that oxidize both NOx and VOCs (Chameides et al., 1988). The NOx–limited and VOC–limited regimes are commonly used to describe whether ozone formation is more controlled by the availability of NOx or peroxy radicals from oxidation of VOCs. HCHO:NO_2 ratios (FNRs) theoretically reflect the relative availability of NO_x and the total organic reactivity to OH. The space-based tropospheric column FNRs can, with caveats (Souri et al., 2023), capture the spatiotemporal evolution of ozone production sensitivity regimes and detect expansion of NOx–limited regimes (Jin et al., 2020; Wang et al., 2021; Johnson et al., 2024). The column FNRs can be converted to surface based FNRs using modelled HCHO and NO_2 within boundary layer and further be used for air pollution indicators (Halla et al., 2011; Jin et al., 2017)

We use FNR to demonstrate the impact of HCHO biases on the model capability to capture the ozone–NOx–VOC chemistry. FNRs calculated with TROPOMI HCHO and NO_2 columns are compared with modelled FNRs using MEGAN isoprene emission and using isoprene emission estimates inferred from CrIS. Figure 5 show that GEOS-Chem can generally capture the monthly FNR distributions but with a negative bias over grasslands and urban areas and a positive bias over forested areas, especially in the Amazon basin. Most regions are NOx-limited over South America, except for urban regions where FNR values are lower than 4 because of high NOx levels in big cities (e.g., São Paulo). Modelled monthly spatial distributions of FNRs determined using isoprene emission estimates from CrIS are more comparable to those determined by TROPOMI data. However, for some regions such as areas along Andes range over Chile, Bolivia and Argentina, GEOS-Chem has a negative bias due to smaller HCHO columns. This is consistent with errors in BVOC emission inventories playing a substantial role in our current ability to determine changes in the oxidizing capacity of the atmosphere above tropical rainforests. Previous studies have proposed column FNR thresholds of 1.0 to 2.0 to describe the transition from NOx–saturated to NOx–limited regimes (Jin and Holloway, 2015). The models reproduce the observed NOx–saturated hotspots over urban areas, where NOx levels are much higher and FNRs are small (< 5). The model using MEGAN isoprene emissions shows high FNRs over forested regions (Fig. 5a), but with a spatial distribution that is different from observations We find isoprene emission estimates inferred from CrIS better reproduce the relatively lower FNRs over the Amazon basin, where the NOx-limited regime can potentially transition to NOx-saturated due to biomass burning.

https://doi.org/10.5194/egusphere-2025-778
Preprint. Discussion started: 26 February 2025
© Author(s) 2025. CC BY 4.0 License.

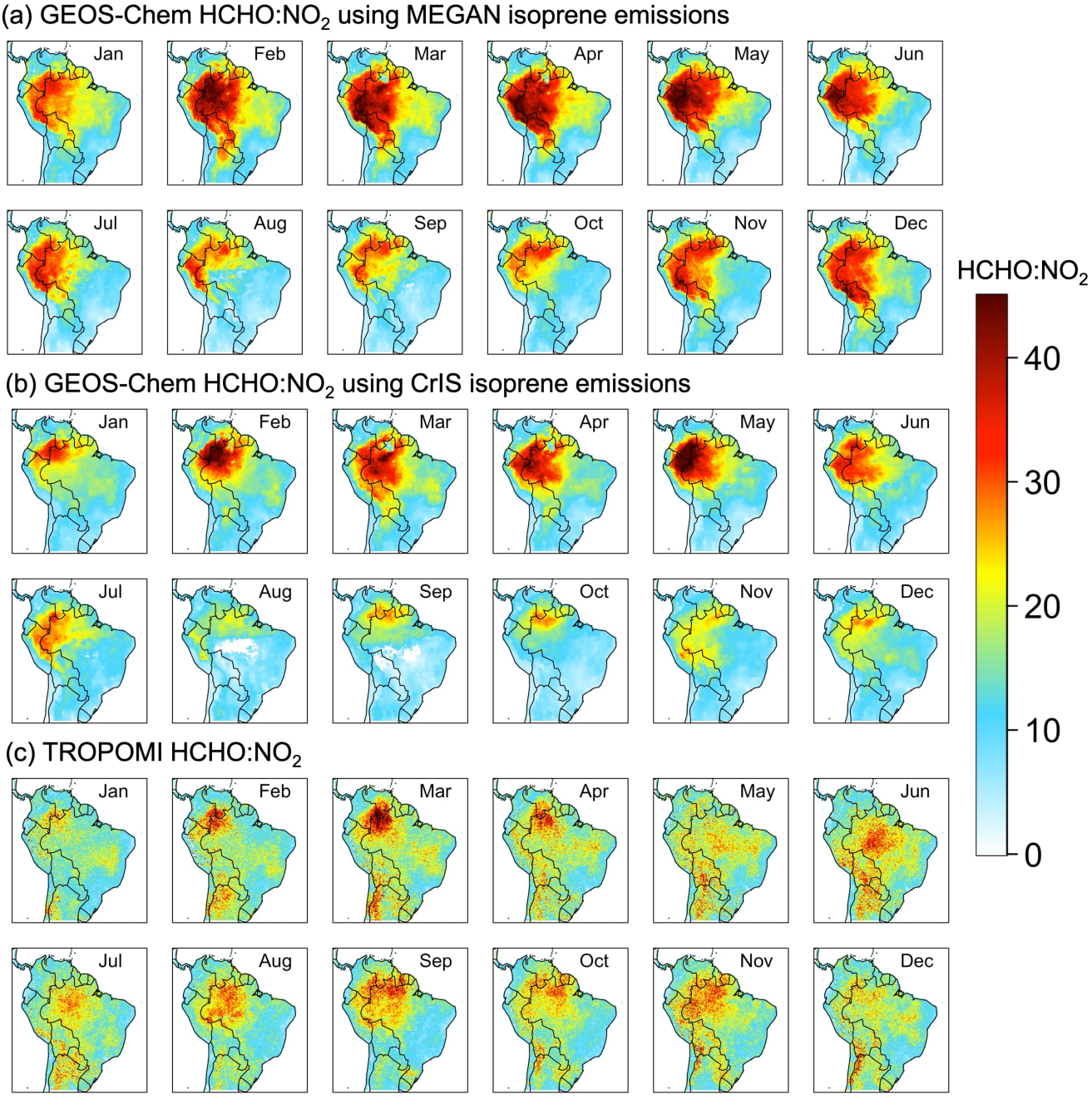

Figure 5: Mean monthly W_{HCHO}: W_{NO2} ratios (FNR; unitless) for year 2019. (a) model simulated FNR with MEGAN isoprene emissions; (b) model simulated FNR with CrIS inferred isoprene emissions; (c) TROPOMI FNR computed using TROPOMI HCHO and NO_2 tropospheric columns.

375

https://doi.org/10.5194/egusphere-2025-778
Preprint. Discussion started: 26 February 2025
© Author(s) 2025. CC BY 4.0 License.

Figure 6 shows that the model using the satellite-inferred isoprene emissions results in higher tropospheric ozone than using MEGAN. Higher predicted ozone is found over the Amazon basin where CrIS inferred isoprene emissions are lower than MEGAN. The model simulates lower ozone to the central and southeast of Brazil where CrIS derived isoprene emissions are higher than MEGAN. We find some increases in ozone around São Paulo where CrIS inferred isoprene emissions are higher than MEGAN. Seguel et al. (2024) examined the trends of ground-level ozone in South American urban areas and found an overall increase due to the reduced NOx levels in the cities. The monthly GEOS-Chem simulated tropospheric ozone columns with CrIS derived isoprene emissions are shown in Fig. S2. We acknowledge that mean differences (0.34 DU) on tropospheric ozone columns over the studied land region due to using different isoprene emission inventories are much smaller than the mean differences (–3.1 DU) between model and satellite observed tropospheric ozone columns (see Fig. S3), which limits our ability to assess any improvement in model performance due to using isoprene emission estimates inferred from CrIS data.

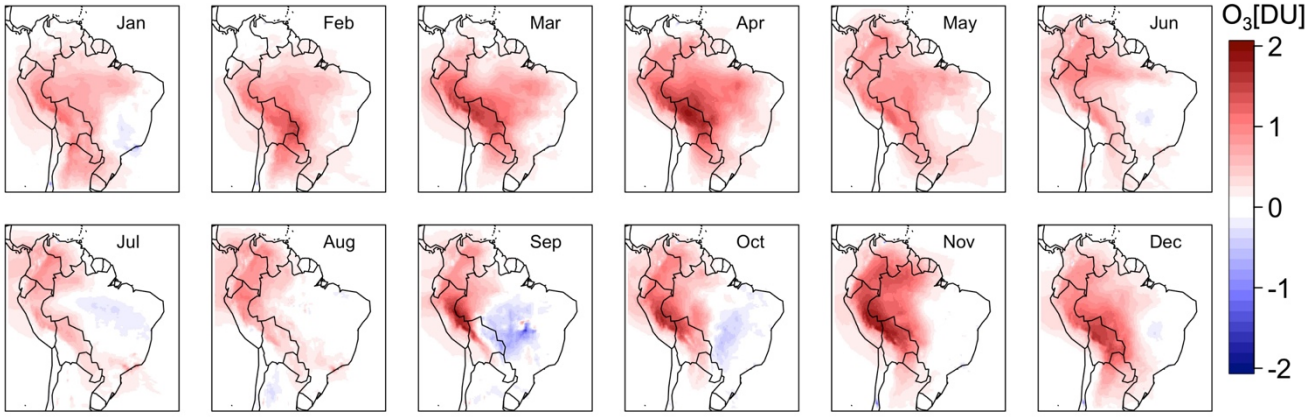

Figure 6: Differences between GEOS-Chem tropospheric ozone simulated with CrIS derived isoprene emissions and MEGAN isoprene emissions for year 2019.

4 Concluding Remarks

Using the GEOS-Chem atmospheric chemistry transport model, we derived top-down isoprene emissions over tropical South America for 2019 using isoprene columns retrieved from CrIS on the NOAA-20 satellite. We found that isoprene emission estimates inferred from CrIS data result in very different spatial and seasonal distributions of isoprene columns over tropical South America than when we use the MEGAN isoprene emission inventory.

We evaluated our CrIS derived isoprene emissions by comparing the corresponding isoprene concentrations with observations collected at the Amazon Tall Tower Observatory, March-December 2019, and found the CrIS derived isoprene emissions reproduce the magnitude of the seasonal cycle better than MEGAN, with smaller monthly biases. The CrIS

https://doi.org/10.5194/egusphere-2025-778
Preprint. Discussion started: 26 February 2025
© Author(s) 2025. CC BY 4.0 License.

derived isoprene emission inventory was evaluated by comparing modelled HCHO distributions based on itself against TROPOMI HCHO. We found that this isoprene emission inventory reduced the annual normalised mean error from 50% to 43%, relative to MEGAN, and reduced the NME from 58% to 47% during the wet season (December – May) and from 36% to 33% for the dry season (July – October). We showed this had positive implications for our ability to reproduce TROPOMI observed HCHO:NO_2 ratios that are indicative of the photochemical environment. We found that the CrIS derived isoprene emissions better reproduced the lower ratio values found over the Amazon basin, where the NOx-limited regime could potentially transition to NOx-saturated due to biomass burning. The resulting changes in tropospheric ozone columns were ±2 DU, with the largest increases over western parts of Amazon basin and lower ozone to the south and east of Brazil, although these changes are small compared to the difference between GEOS-Chem and TROPOMI tropospheric ozone columns.

More accurate estimates of isoprene are of great importance for understanding the relative contribution of anthropogenic and biogenic sources to the formation of ozone and secondary organic aerosol in the upper troposphere (Palmer et al., 2022; Curtius et al., 2024; Shen et al., 2024). Human induced land use and land cover changes have been found to strongly influence isoprene emissions during recent decades compared with those induced by climate change (Chen et al., 2018). Satellite retrievals of isoprene columns, interpreted using state-of-the-art atmospheric chemistry transport models, can help understand some of the impacts on atmospheric composition from, for example, continuing deforestation, widespread drought, and heatwaves. Recent work has shown that these data can also track changes in atmospheric oxidation over forested regions (Shutter et al., 2024). Tracking changes in isoprene over tropical rainforests, in the context of wider land surface quantities, provides a way to check on the health of these remote ecosystems. The Amazon basin has suffered from severe droughts in recent years, associated with deforestation and changes in climate (Bottino et al., 2024; Espinoza et al., 2024). The El Niño-Southern Oscillation has also contributed to droughts in Amazonia, and is predicted to induce more extreme heatwaves and floods over this region in the future (Marengo and Espinoza, 2016). At a time when we are witnessing such extensive and widespread environmental change, particularly across the tropics, it is essential we sustain these important environment datasets (Millet et al., 2024) because they may be one of the first harbingers of an emerging feedback (Spracklen and Coelho, 2023).

Data availability. GEOS-Chem model code and input data are available from the GEOS-Chem website (www.geoschem.org). TROPOMI HCHO and NO_2 data used in this study can be found at https://doi.org/10.5270/S5P-s4ljg54 (Koninklijk Nederlands Meteorologisch Instituut (KNMI), 2018) and https://doi.org/10.5270/S5P-tjlxfd2 (German Aerospace Center (DLR), 2019) respectively. The CrIS isoprene data are to be archived on the Centre for Environmental Data Analysis (CEDA) archive (https://archive.ceda.ac.uk/).

https://doi.org/10.5194/egusphere-2025-778
Preprint. Discussion started: 26 February 2025
© Author(s) 2025. CC BY 4.0 License.

Author contributions. S. S. led the experimental design and the associated model runs and data analysis. P. I. P. helped to design the study and wrote the manuscript with S. S.. All authors helped to revise the manuscript. R. S., B. J. K., and L.V. provided the CrIS isoprene data and the support necessary to apply these data to study isoprene emissions. A. E., A. R., E. Y. P. and J. W. contributed isoprene measurements at ATTO tower.

Competing interests. At least one of the (co-)authors is a member of the editorial board of Atmospheric Chemistry and Physics. The authors have no other competing interests to declare.

Acknowledgements. This research was supported by the UK National Centre for Earth Observation (NCEO) funded by the Natural Environment Research Council (NE/R016518/1).

References

Abbot, D. S., Palmer, P. I., Martin, R. V., Chance, K. V., Jacob, D. J., and Guenther, A.: Seasonal and interannual variability of North American isoprene emissions as determined by formaldehyde column measurements from space, Geophysical Research Letters, 30, 2003GL017336, https://doi.org/10.1029/2003GL017336, 2003.

Andreae, M. O., Acevedo, O. C., Araùjo, A., Artaxo, P., Barbosa, C. G. G., Barbosa, H. M. J., Brito, J., Carbone, S., Chi, X., Cintra, B. B. L., Da Silva, N. F., Dias, N. L., Dias-Júnior, C. Q., Ditas, F., Ditz, R., Godoi, A. F. L., Godoi, R. H. M., Heimann, M., Hoffmann, T., Kesselmeier, J., Könemann, T., Krüger, M. L., Lavric, J. V., Manzi, A. O., Lopes, A. P., Martins, D. L., Mikhailov, E. F., Moran-Zuloaga, D., Nelson, B. W., Nölscher, A. C., Santos Nogueira, D., Piedade, M. T. F., Pöhlker, C., Pöschl, U., Quesada, C. A., Rizzo, L. V., Ro, C.-U., Ruckteschler, N., Sá, L. D. A., De Oliveira Sá, M., Sales, C. B., Dos Santos, R. M. N., Saturno, J., Schöngart, J., Sörgel, M., De Souza, C. M., De Souza, R. A. F., Su, H., Targhetta, N., Tóta, J., Trebs, I., Trumbore, S., Van Eijck, A., Walter, D., Wang, Z., Weber, B., Williams, J., Winderlich, J., Wittmann, F., Wolff, S., and Yáñez-Serrano, A. M.: The Amazon Tall Tower Observatory (ATTO): overview of pilot measurements on ecosystem ecology, meteorology, trace gases, and aerosols, Atmos. Chem. Phys., 15, 10723–10776, https://doi.org/10.5194/acp-15-10723-2015, 2015.

Arneth, A., Monson, R. K., Schurgers, G., Niinemets, Ü., and Palmer, P. I.: Why are estimates of global terrestrial isoprene emissions so similar (and why is this not so for monoterpenes)?, Atmos. Chem. Phys., 8, 4605–4620, https://doi.org/10.5194/acp-8-4605-2008, 2008.

Atkinson, R.: Atmospheric chemistry of VOCs and NOx, Atmospheric Environment, 34, 2063–2101, https://doi.org/10.1016/S1352-2310(99)00460-4, 2000.

Barkley, M. P., Palmer, P. I., Kuhn, U., Kesselmeier, J., Chance, K., Kurosu, T. P., Martin, R. V., Helmig, D., and Guenther, A.: Net ecosystem fluxes of isoprene over tropical South America inferred from Global Ozone Monitoring Experiment (GOME) observations of HCHO columns, J. Geophys. Res., 113, 2008JD009863, https://doi.org/10.1029/2008JD009863, 2008.

Barkley, M. P., Palmer, P. I., De Smedt, I., Karl, T., Guenther, A., and Van Roozendael, M.: Regulated large-scale annual shutdown of Amazonian isoprene emissions?, Geophysical Research Letters, 36, 2008GL036843, https://doi.org/10.1029/2008GL036843, 2009.

https://doi.org/10.5194/egusphere-2025-778
Preprint. Discussion started: 26 February 2025
© Author(s) 2025. CC BY 4.0 License.

Barkley, M. P., Palmer, P. I., Ganzeveld, L., Arneth, A., Hagberg, D., Karl, T., Guenther, A., Paulot, F., Wennberg, P. O., Mao, J., Kurosu, T. P., Chance, K., Müller, J.-F., De Smedt, I., Van Roozendael, M., Chen, D., Wang, Y., and Yantosca, R. M.: Can a "state of the art" chemistry transport model simulate Amazonian tropospheric chemistry?, J. Geophys. Res., 116, D16302, https://doi.org/10.1029/2011JD015893, 2011.

Barkley, M. P., Smedt, I. D., Van Roozendael, M., Kurosu, T. P., Chance, K., Arneth, A., Hagberg, D., Guenther, A., Paulot, F., Marais, E., and Mao, J.: Top-down isoprene emissions over tropical South America inferred from SCIAMACHY and OMI formaldehyde columns, JGR Atmospheres, 118, 6849–6868, https://doi.org/10.1002/jgrd.50552, 2013.

Bates, K. H. and Jacob, D. J.: A new model mechanism for atmospheric oxidation of isoprene: global effects on oxidants, nitrogen oxides, organic products, and secondary organic aerosol, Atmos. Chem. Phys., 19, 9613–9640, https://doi.org/10.5194/acp-19-9613-2019, 2019.

Batista, C. E., Ye, J., Ribeiro, I. O., Guimarães, P. C., Medeiros, A. S. S., Barbosa, R. G., Oliveira, R. L., Duvoisin, S., Jardine, K. J., Gu, D., Guenther, A. B., McKinney, K. A., Martins, L. D., Souza, R. A. F., and Martin, S. T.: Intermediate-scale horizontal isoprene concentrations in the near-canopy forest atmosphere and implications for emission heterogeneity, Proc. Natl. Acad. Sci. U.S.A., 116, 19318–19323, https://doi.org/10.1073/pnas.1904154116, 2019.

Bauwens, M., Stavrakou, T., Müller, J.-F., De Smedt, I., Van Roozendael, M., Van Der Werf, G. R., Wiedinmyer, C., Kaiser, J. W., Sindelarova, K., and Guenther, A.: Nine years of global hydrocarbon emissions based on source inversion of OMI formaldehyde observations, Atmos. Chem. Phys., 16, 10133–10158, https://doi.org/10.5194/acp-16-10133-2016, 2016.

Botía, S., Komiya, S., Marshall, J., Koch, T., Gałkowski, M., Lavric, J., Gomes-Alves, E., Walter, D., Fisch, G., Pinho, D. M., Nelson, B. W., Martins, G., Luijkx, I. T., Koren, G., Florentie, L., Carioca De Araújo, A., Sá, M., Andreae, M. O., Heimann, M., Peters, W., and Gerbig, C.: The CO_2 record at the Amazon Tall Tower Observatory: A new opportunity to study processes on seasonal and inter-annual scales, Global Change Biology, 28, 588–611, https://doi.org/10.1111/gcb.15905, 2022.

Bottino, M. J., Nobre, P., Giarolla, E., Da Silva Junior, M. B., Capistrano, V. B., Malagutti, M., Tamaoki, J. N., De Oliveira, B. F. A., and Nobre, C. A.: Amazon savannization and climate change are projected to increase dry season length and temperature extremes over Brazil, Sci Rep, 14, 5131, https://doi.org/10.1038/s41598-024-55176-5, 2024.

Bourtsoukidis, E., Pozzer, A., Williams, J., Makowski, D., Peñuelas, J., Matthaios, V. N., Lazoglou, G., Yañez-Serrano, A. M., Lelieveld, J., Ciais, P., Vrekoussis, M., Daskalakis, N., and Sciare, J.: High temperature sensitivity of monoterpene emissions from global vegetation, Commun Earth Environ, 5, 23, https://doi.org/10.1038/s43247-023-01175-9, 2024.

Byron, J., Kreuzwieser, J., Purser, G., Van Haren, J., Ladd, S. N., Meredith, L. K., Werner, C., and Williams, J.: Chiral monoterpenes reveal forest emission mechanisms and drought responses, Nature, 609, 307–312, https://doi.org/10.1038/s41586-022-05020-5, 2022.

Carlton, A. G., Wiedinmyer, C., and Kroll, J. H.: A review of Secondary Organic Aerosol (SOA) formation from isoprene, Atmos. Chem. Phys., 9, 4987–5005, https://doi.org/10.5194/acp-9-4987-2009, 2009.

Chameides, W. L., Lindsay, R. W., Richardson, J., and Kiang, C. S.: The Role of Biogenic Hydrocarbons in Urban Photochemical Smog: Atlanta as a Case Study, Science, 241, 1473–1475, https://doi.org/10.1126/science.3420404, 1988.

Chen, W. H., Guenther, A. B., Wang, X. M., Chen, Y. H., Gu, D. S., Chang, M., Zhou, S. Z., Wu, L. L., and Zhang, Y. Q.: Regional to Global Biogenic Isoprene Emission Responses to Changes in Vegetation From 2000 to 2015, JGR Atmospheres, 123, 3757–3771, https://doi.org/10.1002/2017JD027934, 2018.

https://doi.org/10.5194/egusphere-2025-778
Preprint. Discussion started: 26 February 2025
© Author(s) 2025. CC BY 4.0 License.

Claeys, M., Graham, B., Vas, G., Wang, W., Vermeylen, R., Pashynska, V., Cafmeyer, J., Guyon, P., Andreae, M. O., Artaxo, P., and Maenhaut, W.: Formation of Secondary Organic Aerosols Through Photooxidation of Isoprene, Science, 303, 1173–1176, https://doi.org/10.1126/science.1092805, 2004.

Curtius, J., Heinritzi, M., Beck, L. J., Pöhlker, M. L., Tripathi, N., Krumm, B. E., Holzbeck, P., Nussbaumer, C. M., Hernández Pardo, L., Klimach, T., Barmpounis, K., Andersen, S. T., Bardakov, R., Bohn, B., Cecchini, M. A., Chaboureau, J.-P., Dauhut, T., Dienhart, D., Dörich, R., Edtbauer, A., Giez, A., Hartmann, A., Holanda, B. A., Joppe, P., Kaiser, K., Keber, T., Klebach, H., Krüger, O. O., Kürten, A., Mallaun, C., Marno, D., Martinez, M., Monteiro, C., Nelson, C., Ort, L., Raj, S. S., Richter, S., Ringsdorf, A., Rocha, F., Simon, M., Sreekumar, S., Tsokankunku, A., Unfer, G. R., Valenti, I. D., Wang, N., Zahn, A., Zauner-Wieczorek, M., Albrecht, R. I., Andreae, M. O., Artaxo, P., Crowley, J. N., Fischer, H., Harder, H., Herdies, D. L., Machado, L. A. T., Pöhlker, C., Pöschl, U., Possner, A., Pozzer, A., Schneider, J., Williams, J., and Lelieveld, J.: Isoprene nitrates drive new particle formation in Amazon's upper troposphere, Nature, 636, 124–130, https://doi.org/10.1038/s41586-024-08192-4, 2024.

De Smedt, I., Theys, N., Yu, H., Danckaert, T., Lerot, C., Compernolle, S., Van Roozendael, M., Richter, A., Hilboll, A., Peters, E., Pedergnana, M., Loyola, D., Beirle, S., Wagner, T., Eskes, H., Van Geffen, J., Boersma, K. F., and Veefkind, P.: Algorithm theoretical baseline for formaldehyde retrievals from S5P TROPOMI and from the QA4ECV project, Atmos. Meas. Tech., 11, 2395–2426, https://doi.org/10.5194/amt-11-2395-2018, 2018.

De Smedt, I., Romahn, F., and Eichmann, K.-U.: S5P Mission Performance Centre Formaldehyde [L2__HCHO___] Readme, S5P-MPC-BIRA-PRF-HCHO, 2.1, https://sentinels.copernicus.eu/documents/247904/3541451/Sentinel-5P-Formaldehyde-Readme.pdf, 2020.

De Smedt, I., Pinardi, G., Vigouroux, C., Compernolle, S., Bais, A., Benavent, N., Boersma, F., Chan, K.-L., Donner, S., Eichmann, K.-U., Hedelt, P., Hendrick, F., Irie, H., Kumar, V., Lambert, J.-C., Langerock, B., Lerot, C., Liu, C., Loyola, D., Piters, A., Richter, A., Rivera Cárdenas, C., Romahn, F., Ryan, R. G., Sinha, V., Theys, N., Vlietinck, J., Wagner, T., Wang, T., Yu, H., and Van Roozendael, M.: Comparative assessment of TROPOMI and OMI formaldehyde observations and validation against MAX-DOAS network column measurements, Atmos. Chem. Phys., 21, 12561–12593, https://doi.org/10.5194/acp-21-12561-2021, 2021.

DiMaria, C. A., Jones, D. B. A., Worden, H., Bloom, A. A., Bowman, K., Stavrakou, T., Miyazaki, K., Worden, J., Guenther, A., Sarkar, C., Seco, R., Park, J., Tota, J., Alves, E. G., and Ferracci, V.: Optimizing the Isoprene Emission Model MEGAN With Satellite and Ground-Based Observational Constraints, JGR Atmospheres, 128, e2022JD037822, https://doi.org/10.1029/2022JD037822, 2023.

Eastham, S. D., Weisenstein, D. K., and Barrett, S. R. H.: Development and evaluation of the unified tropospheric–stratospheric chemistry extension (UCX) for the global chemistry-transport model GEOS-Chem, Atmospheric Environment, 89, 52–63, https://doi.org/10.1016/j.atmosenv.2014.02.001, 2014.

Eskes, H. J. and Eichmann, K.-U.: S5P Mission Performance Centre Nitrogen Dioxide [L2__NO2___] Readme, S5P-MPC-KNMI-PRF-NO2, 1.6, https://sentinel.esa.int/documents/247904/3541451/Sentinel-5P-Nitrogen-Dioxide-Level-2-Product-Readme-File, 2022.

Espinoza, J.-C., Jimenez, J. C., Marengo, J. A., Schongart, J., Ronchail, J., Lavado-Casimiro, W., and Ribeiro, J. V. M.: The new record of drought and warmth in the Amazon in 2023 related to regional and global climatic features, Sci Rep, 14, 8107, https://doi.org/10.1038/s41598-024-58782-5, 2024.

Feng, L., Palmer, P. I., Parker, R. J., Lunt, M. F., and Bösch, H.: Methane emissions are predominantly responsible for record-breaking atmospheric methane growth rates in 2020 and 2021, Atmos. Chem. Phys., 23, 4863–4880, https://doi.org/10.5194/acp-23-4863-2023, 2023.

https://doi.org/10.5194/egusphere-2025-778
Preprint. Discussion started: 26 February 2025
© Author(s) 2025. CC BY 4.0 License.

Feng, S., Jiang, F., Qian, T., Wang, N., Jia, M., Zheng, S., Chen, J., Ying, F., and Ju, W.: Constraining non-methane VOC emissions with TROPOMI HCHO observations: impact on summertime ozone simulation in August 2022 in China, Atmos. Chem. Phys., 24, 7481–7498, https://doi.org/10.5194/acp-24-7481-2024, 2024.

Ferracci, V., Bolas, C. G., Freshwater, R. A., Staniaszek, Z., King, T., Jaars, K., Otu-Larbi, F., Beale, J., Malhi, Y., Waine, T. W., Jones, R. L., Ashworth, K., and Harris, N. R. P.: Continuous Isoprene Measurements in a UK Temperate Forest for a Whole Growing Season: Effects of Drought Stress During the 2018 Heatwave, Geophysical Research Letters, 47, e2020GL088885, https://doi.org/10.1029/2020GL088885, 2020.

Ferracci, V., Weber, J., Bolas, C. G., Robinson, A. D., Tummon, F., Rodríguez-Ros, P., Cortés-Greus, P., Baccarini, A., Jones, R. L., Galí, M., Simó, R., Schmale, J., and Harris, Neil. R. P.: Atmospheric isoprene measurements reveal larger-than-expected Southern Ocean emissions, Nat Commun, 15, 2571, https://doi.org/10.1038/s41467-024-46744-4, 2024.

Fini, A., Brunetti, C., Loreto, F., Centritto, M., Ferrini, F., and Tattini, M.: Isoprene Responses and Functions in Plants Challenged by Environmental Pressures Associated to Climate Change, Front. Plant Sci., 8, 1281, https://doi.org/10.3389/fpls.2017.01281, 2017.

Fu, D., Millet, D. B., Wells, K. C., Payne, V. H., Yu, S., Guenther, A., and Eldering, A.: Direct retrieval of isoprene from satellite-based infrared measurements, Nat Commun, 10, 3811, https://doi.org/10.1038/s41467-019-11835-0, 2019.

Fuchs, H., Hofzumahaus, A., Rohrer, F., Bohn, B., Brauers, T., Dorn, H.-P., Häseler, R., Holland, F., Kaminski, M., Li, X., Lu, K., Nehr, S., Tillmann, R., Wegener, R., and Wahner, A.: Experimental evidence for efficient hydroxyl radical regeneration in isoprene oxidation, Nature Geosci, 6, 1023–1026, https://doi.org/10.1038/ngeo1964, 2013.

Giglio, L., Schroeder, W., Hall, J. V., and Justice, C. O.: MODIS Collection 6 Active Fire Product User's Guide, Revision C, NASA, https://modis-fire.umd.edu/files/MODIS_C6_Fire_User_Guide_C.pdf, 2020.

Gomes Alves, E., Aquino Santana, R., Quaresma Dias-Júnior, C., Botía, S., Taylor, T., Yáñez-Serrano, A. M., Kesselmeier, J., Bourtsoukidis, E., Williams, J., Lembo Silveira De Assis, P. I., Martins, G., De Souza, R., Duvoisin Júnior, S., Guenther, A., Gu, D., Tsokankunku, A., Sörgel, M., Nelson, B., Pinto, D., Komiya, S., Martins Rosa, D., Weber, B., Barbosa, C., Robin, M., Feeley, K. J., Duque, A., Londoño Lemos, V., Contreras, M. P., Idarraga, A., López, N., Husby, C., Jestrow, B., and Cely Toro, I. M.: Intra- and interannual changes in isoprene emission from central Amazonia, Atmos. Chem. Phys., 23, 8149–8168, https://doi.org/10.5194/acp-23-8149-2023, 2023.

Gonzi, S., Palmer, P. I., Barkley, M. P., De Smedt, I., and Van Roozendael, M.: Biomass burning emission estimates inferred from satellite column measurements of HCHO: Sensitivity to co-emitted aerosol and injection height: HCHO BIOMASS BURNING EMISSIONS, Geophys. Res. Lett., 38, n/a-n/a, https://doi.org/10.1029/2011GL047890, 2011.

Gu, D., Guenther, A. B., Shilling, J. E., Yu, H., Huang, M., Zhao, C., Yang, Q., Martin, S. T., Artaxo, P., Kim, S., Seco, R., Stavrakou, T., Longo, K. M., Tóta, J., De Souza, R. A. F., Vega, O., Liu, Y., Shrivastava, M., Alves, E. G., Santos, F. C., Leng, G., and Hu, Z.: Airborne observations reveal elevational gradient in tropical forest isoprene emissions, Nat Commun, 8, 15541, https://doi.org/10.1038/ncomms15541, 2017.

Guenther, A., Karl, T., Harley, P., Wiedinmyer, C., Palmer, P. I., and Geron, C.: Estimates of global terrestrial isoprene emissions using MEGAN (Model of Emissions of Gases and Aerosols from Nature), Atmos. Chem. Phys., 2006.

Guenther, A. B., Jiang, X., Heald, C. L., Sakulyanontvittaya, T., Duhl, T., Emmons, L. K., and Wang, X.: The Model of Emissions of Gases and Aerosols from Nature version 2.1 (MEGAN2.1): an extended and updated framework for modeling biogenic emissions, Geosci. Model Dev., 5, 1471–1492, https://doi.org/10.5194/gmd-5-1471-2012, 2012.

https://doi.org/10.5194/egusphere-2025-778
Preprint. Discussion started: 26 February 2025
© Author(s) 2025. CC BY 4.0 License.

Halla, J. D., Wagner, T., Beirle, S., Brook, J. R., Hayden, K. L., O'Brien, J. M., Ng, A., Majonis, D., Wenig, M. O., and McLaren, R.: Determination of tropospheric vertical columns of NO₂ and aerosol optical properties in a rural setting using MAX-DOAS, Atmos. Chem. Phys., 11, 12475–12498, https://doi.org/10.5194/acp-11-12475-2011, 2011.

Hansen, R. F., Lewis, T. R., Graham, L., Whalley, L. K., Seakins, P. W., Heard, D. E., and Blitz, M. A.: OH production from the photolysis of isoprene-derived peroxy radicals: cross-sections, quantum yields and atmospheric implications, Phys. Chem. Chem. Phys., 19, 2332–2345, https://doi.org/10.1039/C6CP06718B, 2017.

Hoesly, R. M., Smith, S. J., Feng, L., Klimont, Z., Janssens-Maenhout, G., Pitkanen, T., Seibert, J. J., Vu, L., Andres, R. J., Bolt, R. M., Bond, T. C., Dawidowski, L., Kholod, N., Kurokawa, J., Li, M., Liu, L., Lu, Z., Moura, M. C. P., O'Rourke, P. R., and Zhang, Q.: Historical (1750–2014) anthropogenic emissions of reactive gases and aerosols from the Community Emissions Data System (CEDS), Geosci. Model Dev., 11, 369–408, https://doi.org/10.5194/gmd-11-369-2018, 2018.

Hofzumahaus, A., Rohrer, F., Lu, K., Bohn, B., Brauers, T., Chang, C.-C., Fuchs, H., Holland, F., Kita, K., Kondo, Y., Li, X., Lou, S., Shao, M., Zeng, L., Wahner, A., and Zhang, Y.: Amplified Trace Gas Removal in the Troposphere, Science, 324, 1702–1704, https://doi.org/10.1126/science.1164566, 2009.

Huang, L., McGaughey, G., McDonald-Buller, E., Kimura, Y., and Allen, D. T.: Quantifying regional, seasonal and interannual contributions of environmental factors on isoprene and monoterpene emissions estimates over eastern Texas, Atmospheric Environment, 106, 120–128, https://doi.org/10.1016/j.atmosenv.2015.01.072, 2015.

Jiang, X., Guenther, A., Potosnak, M., Geron, C., Seco, R., Karl, T., Kim, S., Gu, L., and Pallardy, S.: Isoprene emission response to drought and the impact on global atmospheric chemistry, Atmospheric Environment, 183, 69–83, https://doi.org/10.1016/j.atmosenv.2018.01.026, 2018.

Jin, X. and Holloway, T.: Spatial and temporal variability of ozone sensitivity over China observed from the Ozone Monitoring Instrument, JGR Atmospheres, 120, 7229–7246, https://doi.org/10.1002/2015JD023250, 2015.

Jin, X., Fiore, A. M., Murray, L. T., Valin, L. C., Lamsal, L. N., Duncan, B., Folkert Boersma, K., De Smedt, I., Abad, G. G., Chance, K., and Tonnesen, G. S.: Evaluating a Space-Based Indicator of Surface Ozone-NO_x-VOC Sensitivity Over Midlatitude Source Regions and Application to Decadal Trends, JGR Atmospheres, 122, https://doi.org/10.1002/2017JD026720, 2017.

Jin, X., Fiore, A., Boersma, K. F., Smedt, I. D., and Valin, L.: Inferring Changes in Summertime Surface Ozone–NO_x–VOC Chemistry over U.S. Urban Areas from Two Decades of Satellite and Ground-Based Observations, Environ. Sci. Technol., 54, 6518–6529, https://doi.org/10.1021/acs.est.9b07785, 2020.

Johnson, M. S., Philip, S., Meech, S., Kumar, R., Sorek-Hamer, M., Shiga, Y. P., and Jung, J.: Insights into the long-term (2005–2021) spatiotemporal evolution of summer ozone production sensitivity in the Northern Hemisphere derived with the Ozone Monitoring Instrument (OMI), Atmos. Chem. Phys., 24, 10363–10384, https://doi.org/10.5194/acp-24-10363-2024, 2024.

Kaiser, J., Jacob, D. J., Zhu, L., Travis, K. R., Fisher, J. A., González Abad, G., Zhang, L., Zhang, X., Fried, A., Crounse, J. D., St. Clair, J. M., and Wisthaler, A.: High-resolution inversion of OMI formaldehyde columns to quantify isoprene emission on ecosystem-relevant scales: application to the southeast US, Atmos. Chem. Phys., 18, 5483–5497, https://doi.org/10.5194/acp-18-5483-2018, 2018.

Kesselmeier, J. and Staudt, M.: Biogenic Volatile Organic Compounds (VOC): An Overview on Emission, Physiology and Ecology, Journal of Atmospheric Chemistry, 33, 23–88, https://doi.org/10.1023/A:1006127516791, 1999.

https://doi.org/10.5194/egusphere-2025-778
Preprint. Discussion started: 26 February 2025
© Author(s) 2025. CC BY 4.0 License.

Kroll, J. H., Ng, N. L., Murphy, S. M., Flagan, R. C., and Seinfeld, J. H.: Secondary organic aerosol formation from isoprene photooxidation under high-NO $_x$ conditions, Geophysical Research Letters, 32, 2005GL023637, https://doi.org/10.1029/2005GL023637, 2005.

Kroll, J. H., Ng, N. L., Murphy, S. M., Flagan, R. C., and Seinfeld, J. H.: Secondary Organic Aerosol Formation from Isoprene Photooxidation, Environ. Sci. Technol., 40, 1869–1877, https://doi.org/10.1021/es0524301, 2006.

Lelieveld, J., Butler, T. M., Crowley, J. N., Dillon, T. J., Fischer, H., Ganzeveld, L., Harder, H., Lawrence, M. G., Martinez, M., Taraborrelli, D., and Williams, J.: Atmospheric oxidation capacity sustained by a tropical forest, Nature, 452, 737–740, https://doi.org/10.1038/nature06870, 2008.

Marais, E. A., Jacob, D. J., Kurosu, T. P., Chance, K., Murphy, J. G., Reeves, C., Mills, G., Casadio, S., Millet, D. B., Barkley, M. P., Paulot, F., and Mao, J.: Isoprene emissions in Africa inferred from OMI observations of formaldehyde columns, Atmos. Chem. Phys., 12, 6219–6235, https://doi.org/10.5194/acp-12-6219-2012, 2012.

Marais, E. A., Jacob, D. J., Jimenez, J. L., Campuzano-Jost, P., Day, D. A., Hu, W., Krechmer, J., Zhu, L., Kim, P. S., Miller, C. C., Fisher, J. A., Travis, K., Yu, K., Hanisco, T. F., Wolfe, G. M., Arkinson, H. L., Pye, H. O. T., Froyd, K. D., Liao, J., and McNeill, V. F.: Aqueous-phase mechanism for secondary organic aerosol formation from isoprene: application to the southeast United States and co-benefit of SO₂ emission controls, Atmos. Chem. Phys., 16, 1603–1618, https://doi.org/10.5194/acp-16-1603-2016, 2016.

Marengo, J. A. and Espinoza, J. C.: Extreme seasonal droughts and floods in Amazonia: causes, trends and impacts, Intl Journal of Climatology, 36, 1033–1050, https://doi.org/10.1002/joc.4420, 2016.

Marvin, M. R., Wolfe, G. M., Salawitch, R. J., Canty, T. P., Roberts, S. J., Travis, K. R., Aikin, K. C., De Gouw, J. A., Graus, M., Hanisco, T. F., Holloway, J. S., Hübler, G., Kaiser, J., Keutsch, F. N., Peischl, J., Pollack, I. B., Roberts, J. M., Ryerson, T. B., Veres, P. R., and Warneke, C.: Impact of evolving isoprene mechanisms on simulated formaldehyde: An inter-comparison supported by in situ observations from SENEX, Atmospheric Environment, 164, 325–336, https://doi.org/10.1016/j.atmosenv.2017.05.049, 2017.

Mayhew, A. W., Edwards, P. M., and Hamilton, J. F.: Daytime isoprene nitrates under changing NO_x and O_3, Atmos. Chem. Phys., 23, 8473–8485, https://doi.org/10.5194/acp-23-8473-2023, 2023.

Millet, D. B., Jacob, D. J., Boersma, K. F., Fu, T., Kurosu, T. P., Chance, K., Heald, C. L., and Guenther, A.: Spatial distribution of isoprene emissions from North America derived from formaldehyde column measurements by the OMI satellite sensor, J. Geophys. Res., 113, 2007JD008950, https://doi.org/10.1029/2007JD008950, 2008.

Millet, D. B., Baasandorj, M., Hu, L., Mitroo, D., Turner, J., and Williams, B. J.: Nighttime Chemistry and Morning Isoprene Can Drive Urban Ozone Downwind of a Major Deciduous Forest, Environ. Sci. Technol., 50, 4335–4342, https://doi.org/10.1021/acs.est.5b06367, 2016.

Millet, D. B., Palmer, P. I., Levelt, P. F., Gallardo, L., and Shikwambana, L.: Coordinated Geostationary, Multispectral Satellite Observations Are Critical for Climate and Air Quality Progress, AGU Advances, 5, e2024AV001322, https://doi.org/10.1029/2024AV001322, 2024.

Misztal, P. K., Avise, J. C., Karl, T., Scott, K., Jonsson, H. H., Guenther, A. B., and Goldstein, A. H.: Evaluation of regional isoprene emission factors and modeled fluxes in California, Atmos. Chem. Phys., 16, 9611–9628, https://doi.org/10.5194/acp-16-9611-2016, 2016.

https://doi.org/10.5194/egusphere-2025-778
Preprint. Discussion started: 26 February 2025
© Author(s) 2025. CC BY 4.0 License.

Miyoshi, A., Hatakeyama, S., and Washida, N.: OH radical- initiated photooxidation of isoprene: An estimate of global CO production, J. Geophys. Res., 99, 18779–18787, https://doi.org/10.1029/94JD01334, 1994.

Monson, R. K., Jaeger, C. H., Adams, W. W., Driggers, E. M., Silver, G. M., and Fall, R.: Relationships among Isoprene Emission Rate, Photosynthesis, and Isoprene Synthase Activity as Influenced by Temperature, Plant Physiol., 98, 1175–1180, https://doi.org/10.1104/pp.98.3.1175, 1992.

Monson, R. K., Jones, R. T., Rosenstiel, T. N., and Schnitzler, J.: Why only some plants emit isoprene, Plant Cell & Environment, 36, 503–516, https://doi.org/10.1111/pce.12015, 2013.

Müller, J.-F., Stavrakou, T., Wallens, S., De Smedt, I., Van Roozendael, M., Potosnak, M. J., Rinne, J., Munger, B., Goldstein, A., and Guenther, A. B.: Global isoprene emissions estimated using MEGAN, ECMWF analyses and a detailed canopy environment model, Atmos. Chem. Phys., 8, 1329–1341, https://doi.org/10.5194/acp-8-1329-2008, 2008.

Müller, J.-F., Stavrakou, T., Oomen, G.-M., Opacka, B., De Smedt, I., Guenther, A., Vigouroux, C., Langerock, B., Aquino, C. A. B., Grutter, M., Hannigan, J., Hase, F., Kivi, R., Lutsch, E., Mahieu, E., Makarova, M., Metzger, J.-M., Morino, I., Murata, I., Nagahama, T., Notholt, J., Ortega, I., Palm, M., Röhling, A., Stremme, W., Strong, K., Sussmann, R., Té, Y., and Fried, A.: Bias correction of OMI HCHO columns based on FTIR and aircraft measurements and impact on top-down emission estimates, Atmos. Chem. Phys., 24, 2207–2237, https://doi.org/10.5194/acp-24-2207-2024, 2024.

Nölscher, A. C., Yañez-Serrano, A. M., Wolff, S., De Araujo, A. C., Lavrič, J. V., Kesselmeier, J., and Williams, J.: Unexpected seasonality in quantity and composition of Amazon rainforest air reactivity, Nat Commun, 7, 10383, https://doi.org/10.1038/ncomms10383, 2016.

Opacka, B., Müller, J.-F., Stavrakou, T., Bauwens, M., Sindelarova, K., Markova, J., and Guenther, A. B.: Global and regional impacts of land cover changes on isoprene emissions derived from spaceborne data and the MEGAN model, Atmos. Chem. Phys., 21, 8413–8436, https://doi.org/10.5194/acp-21-8413-2021, 2021.

Opacka, B., Stavrakou, T., Müller, J.-F., De Smedt, I., Van Geffen, J., Marais, E. A., Horner, R. P., Millet, D. B., Wells, K. C., and Guenther, A. B.: Natural emissions of VOC and NO_x over Africa constrained by TROPOMI HCHO and NO_2 data using the MAGRITTEv1.1 model, https://doi.org/10.5194/egusphere-2024-2912, 27 September 2024.

Palmer, P. I., Jacob, D. J., Fiore, A. M., Martin, R. V., Chance, K., and Kurosu, T. P.: Mapping isoprene emissions over North America using formaldehyde column observations from space, J. Geophys. Res., 108, 2002JD002153, https://doi.org/10.1029/2002JD002153, 2003.

Palmer, P. I., Abbot, D. S., Fu, T., Jacob, D. J., Chance, K., Kurosu, T. P., Guenther, A., Wiedinmyer, C., Stanton, J. C., Pilling, M. J., Pressley, S. N., Lamb, B., and Sumner, A. L.: Quantifying the seasonal and interannual variability of North American isoprene emissions using satellite observations of the formaldehyde column, J. Geophys. Res., 111, 2005JD006689, https://doi.org/10.1029/2005JD006689, 2006.

Palmer, P. I., Barkley, M. P., Kurosu, T. P., Lewis, A. C., Saxton, J. E., Chance, K., and Gatti, L. V.: Interpreting satellite column observations of formaldehyde over tropical South America, Phil. Trans. R. Soc. A., 365, 1741–1751, https://doi.org/10.1098/rsta.2007.2042, 2007.

Palmer, P. I., Marvin, M. R., Siddans, R., Kerridge, B. J., and Moore, D. P.: Nocturnal survival of isoprene linked to formation of upper tropospheric organic aerosol, Science, 375, 562–566, https://doi.org/10.1126/science.abg4506, 2022.

Pfannerstill, E. Y., Reijrink, N. G., Edtbauer, A., Ringsdorf, A., Zannoni, N., Araújo, A., Ditas, F., Holanda, B. A., Sá, M. O., Tsokankunku, A., Walter, D., Wolff, S., Lavrič, J. V., Pöhlker, C., Sörgel, M., and Williams, J.: Total OH reactivity over

© Author(s) 2025. CC BY 4.0 License.

the Amazon rainforest: variability with temperature, wind, rain, altitude, time of day, season, and an overall budget closure, Atmos. Chem. Phys., 21, 6231–6256, https://doi.org/10.5194/acp-21-6231-2021, 2021.

Pye, H. O. T., Chan, A. W. H., Barkley, M. P., and Seinfeld, J. H.: Global modeling of organic aerosol: the importance of reactive nitrogen (NO_x and NO₃), Atmos. Chem. Phys., 10, 11261–11276, https://doi.org/10.5194/acp-10-11261-2010, 2010.

Ringsdorf, A., Edtbauer, A., Vilà-Guerau De Arellano, J., Pfannerstill, E. Y., Gromov, S., Kumar, V., Pozzer, A., Wolff, S., Tsokankunku, A., Soergel, M., Sá, M. O., Araújo, A., Ditas, F., Poehlker, C., Lelieveld, J., and Williams, J.: Inferring the diurnal variability of OH radical concentrations over the Amazon from BVOC measurements, Sci Rep, 13, 14900, https://doi.org/10.1038/s41598-023-41748-4, 2023.

Sahu, A., Mostofa, M. G., Weraduwage, S. M., and Sharkey, T. D.: Hydroxymethylbutenyl diphosphate accumulation reveals MEP pathway regulation for high CO_2 -induced suppression of isoprene emission, Proc. Natl. Acad. Sci. U.S.A., 120, e2309536120, https://doi.org/10.1073/pnas.2309536120, 2023.

Sarkar, C., Guenther, A. B., Park, J.-H., Seco, R., Alves, E., Batalha, S., Santana, R., Kim, S., Smith, J., Tóta, J., and Vega, O.: PTR-TOF-MS eddy covariance measurements of isoprene and monoterpene fluxes from an eastern Amazonian rainforest, Atmos. Chem. Phys., 20, 7179–7191, https://doi.org/10.5194/acp-20-7179-2020, 2020.

Saunier, A., Ormeño, E., Piga, D., Armengaud, A., Boissard, C., Lathière, J., Szopa, S., Genard-Zielinski, A.-C., and Fernandez, C.: Isoprene contribution to ozone production under climate change conditions in the French Mediterranean area, Reg Environ Change, 20, 111, https://doi.org/10.1007/s10113-020-01697-4, 2020.

Seco, R., Karl, T., Guenther, A., Hosman, K. P., Pallardy, S. G., Gu, L., Geron, C., Harley, P., and Kim, S.: Ecosystem-scale volatile organic compound fluxes during an extreme drought in a broadleaf temperate forest of the Missouri Ozarks (central USA), Global Change Biology, 21, 3657–3674, https://doi.org/10.1111/gcb.12980, 2015.

Seco, R., Holst, T., Davie-Martin, C. L., Simin, T., Guenther, A., Pirk, N., Rinne, J., and Rinnan, R.: Strong isoprene emission response to temperature in tundra vegetation, Proc. Natl. Acad. Sci. U.S.A., 119, e2118014119, https://doi.org/10.1073/pnas.2118014119, 2022.

Seguel, R. J., Castillo, L., Opazo, C., Rojas, N. Y., Nogueira, T., Cazorla, M., Gavidia-Calderón, M., Gallardo, L., Garreaud, R., Carrasco-Escaff, T., and Elshorbany, Y.: Changes in South American surface ozone trends: exploring the influences of precursors and extreme events, Atmos. Chem. Phys., 24, 8225–8242, https://doi.org/10.5194/acp-24-8225-2024, 2024.

Sharkey, T. D., Wiberley, A. E., and Donohue, A. R.: Isoprene Emission from Plants: Why and How, Annals of Botany, 101, 5–18, https://doi.org/10.1093/aob/mcm240, 2007.

Shen, J., Russell, D. M., DeVivo, J., Kunkler, F., Baalbaki, R., Mentler, B., Scholz, W., Yu, W., Caudillo-Plath, L., Sommer, E., Ahongshangbam, E., Alfaouri, D., Almeida, J., Amorim, A., Beck, L. J., Beckmann, H., Berntheusel, M., Bhattacharyya, N., Canagaratna, M. R., Chassaing, A., Cruz-Simbron, R., Dada, L., Duplissy, J., Gordon, H., Granzin, M., Große Schute, L., Heinritzi, M., Iyer, S., Klebach, H., Krüger, T., Kürten, A., Lampimäki, M., Liu, L., Lopez, B., Martinez, M., Morawiec, A., Onnela, A., Peltola, M., Rato, P., Reza, M., Richter, S., Rörup, B., Sebastian, M. K., Simon, M., Surdu, M., Tamme, K., Thakur, R. C., Tomé, A., Tong, Y., Top, J., Umo, N. S., Unfer, G., Vettikkat, L., Weissbacher, J., Xenofontos, C., Yang, B., Zauner-Wieczorek, M., Zhang, J., Zheng, Z., Baltensperger, U., Christoudias, T., Flagan, R. C., El Haddad, I., Junninen, H., Möhler, O., Riipinen, I., Rohner, U., Schobesberger, S., Volkamer, R., Winkler, P. M., Hansel, A., Lehtipalo, K., Donahue, N. M., Lelieveld, J., Harder, H., Kulmala, M., Worsnop, D. R., Kirkby, J., Curtius, J., and He, X.-C.: New particle formation from isoprene under upper-tropospheric conditions, Nature, 636, 115–123, https://doi.org/10.1038/s41586-024-08196-0, 2024.

https://doi.org/10.5194/egusphere-2025-778
Preprint. Discussion started: 26 February 2025
© Author(s) 2025. CC BY 4.0 License.

Shim, C., Wang, Y., Choi, Y., Palmer, P. I., Abbot, D. S., and Chance, K.: Constraining global isoprene emissions with Global Ozone Monitoring Experiment (GOME) formaldehyde column measurements, J. Geophys. Res., 110, 2004JD005629, https://doi.org/10.1029/2004JD005629, 2005.

Shutter, J. D., Millet, D. B., Wells, K. C., Payne, V. H., Nowlan, C. R., and Abad, G. G.: Interannual changes in atmospheric oxidation over forests determined from space, Sci. Adv., 10, eadn1115, https://doi.org/10.1126/sciadv.adn1115, 2024.

Souri, A. H., Johnson, M. S., Wolfe, G. M., Crawford, J. H., Fried, A., Wisthaler, A., Brune, W. H., Blake, D. R., Weinheimer, A. J., Verhoelst, T., Compernolle, S., Pinardi, G., Vigouroux, C., Langerock, B., Choi, S., Lamsal, L., Zhu, L., Sun, S., Cohen, R. C., Min, K.-E., Cho, C., Philip, S., Liu, X., and Chance, K.: Characterization of errors in satellite-based HCHO / NO_2 tropospheric column ratios with respect to chemistry, column-to-PBL translation, spatial representation, and retrieval uncertainties, Atmos. Chem. Phys., 23, 1963–1986, https://doi.org/10.5194/acp-23-1963-2023, 2023.

Spracklen, D. V. and Coelho, C. A. S.: Modeling early warning signs of possible Amazon Forest dieback, Sci. Adv., 9, eadk5670, https://doi.org/10.1126/sciadv.adk5670, 2023.

Stavrakou, T., Müller, J.-F., De Smedt, I., Van Roozendael, M., Van Der Werf, G. R., Giglio, L., and Guenther, A.: Evaluating the performance of pyrogenic and biogenic emission inventories against one decade of space-based formaldehyde columns, Atmos. Chem. Phys., 9, 1037–1060, https://doi.org/10.5194/acp-9-1037-2009, 2009.

Stavrakou, T., Müller, J.-F., Bauwens, M., De Smedt, I., Van Roozendael, M., Guenther, A., Wild, M., and Xia, X.: Isoprene emissions over Asia 1979–2012: impact of climate and land-use changes, Atmos. Chem. Phys., 14, 4587–4605, https://doi.org/10.5194/acp-14-4587-2014, 2014.

Surl, L., Palmer, P. I., and González Abad, G.: Which processes drive observed variations of HCHO columns over India?, Atmos. Chem. Phys., 18, 4549–4566, https://doi.org/10.5194/acp-18-4549-2018, 2018.

Taylor, T. C., McMahon, S. M., Smith, M. N., Boyle, B., Violle, C., Van Haren, J., Simova, I., Meir, P., Ferreira, L. V., De Camargo, P. B., Da Costa, A. C. L., Enquist, B. J., and Saleska, S. R.: Isoprene emission structures tropical tree biogeography and community assembly responses to climate, New Phytologist, 220, 435–446, https://doi.org/10.1111/nph.15304, 2018.

Van Der Werf, G. R., Randerson, J. T., Giglio, L., Van Leeuwen, T. T., Chen, Y., Rogers, B. M., Mu, M., Van Marle, M. J. E., Morton, D. C., Collatz, G. J., Yokelson, R. J., and Kasibhatla, P. S.: Global fire emissions estimates during 1997–2016, Earth Syst. Sci. Data, 9, 697–720, https://doi.org/10.5194/essd-9-697-2017, 2017.

Van Geffen, J., Eskes, H., Compernolle, S., Pinardi, G., Verhoelst, T., Lambert, J.-C., Sneep, M., Ter Linden, M., Ludewig, A., Boersma, K. F., and Veefkind, J. P.: Sentinel-5P TROPOMI NO₂ retrieval: impact of version v2.2 improvements and comparisons with OMI and ground-based data, Atmos. Meas. Tech., 15, 2037–2060, https://doi.org/10.5194/amt-15-2037-2022, 2022.

Veefkind, J. P., Aben, I., McMullan, K., Förster, H., De Vries, J., Otter, G., Claas, J., Eskes, H. J., De Haan, J. F., Kleipool, Q., Van Weele, M., Hasekamp, O., Hoogeveen, R., Landgraf, J., Snel, R., Tol, P., Ingmann, P., Voors, R., Kruizinga, B., Vink, R., Visser, H., and Levelt, P. F.: TROPOMI on the ESA Sentinel-5 Precursor: A GMES mission for global observations of the atmospheric composition for climate, air quality and ozone layer applications, Remote Sensing of Environment, 120, 70–83, https://doi.org/10.1016/j.rse.2011.09.027, 2012.

Vigouroux, C., Langerock, B., Bauer Aquino, C. A., Blumenstock, T., Cheng, Z., De Mazière, M., De Smedt, I., Grutter, M., Hannigan, J. W., Jones, N., Kivi, R., Loyola, D., Lutsch, E., Mahieu, E., Makarova, M., Metzger, J.-M., Morino, I., Murata, I., Nagahama, T., Notholt, J., Ortega, I., Palm, M., Pinardi, G., Röhling, A., Smale, D., Stremme, W., Strong, K., Sussmann,

https://doi.org/10.5194/egusphere-2025-778
Preprint. Discussion started: 26 February 2025
© Author(s) 2025. CC BY 4.0 License.

R., Té, Y., Van Roozendael, M., Wang, P., and Winkler, H.: TROPOMI–Sentinel-5 Precursor formaldehyde validation using an extensive network of ground-based Fourier-transform infrared stations, Atmos. Meas. Tech., 13, 3751–3767, https://doi.org/10.5194/amt-13-3751-2020, 2020.

Wang, P., Schade, G., Estes, M., and Ying, Q.: Improved MEGAN predictions of biogenic isoprene in the contiguous United States, Atmospheric Environment, 148, 337–351, https://doi.org/10.1016/j.atmosenv.2016.11.006, 2017.

Wang, W., Van Der A, R., Ding, J., Van Weele, M., and Cheng, T.: Spatial and temporal changes of the ozone sensitivity in China based on satellite and ground-based observations, Atmos. Chem. Phys., 21, 7253–7269, https://doi.org/10.5194/acp-21-7253-2021, 2021.

Warneke, C., De Gouw, J. A., Del Negro, L., Brioude, J., McKeen, S., Stark, H., Kuster, W. C., Goldan, P. D., Trainer, M., Fehsenfeld, F. C., Wiedinmyer, C., Guenther, A. B., Hansel, A., Wisthaler, A., Atlas, E., Holloway, J. S., Ryerson, T. B., Peischl, J., Huey, L. G., and Hanks, A. T. C.: Biogenic emission measurement and inventories determination of biogenic emissions in the eastern United States and Texas and comparison with biogenic emission inventories, J. Geophys. Res., 115, 2009JD012445, https://doi.org/10.1029/2009JD012445, 2010.

Wells, K. C., Millet, D. B., Payne, V. H., Deventer, M. J., Bates, K. H., De Gouw, J. A., Graus, M., Warneke, C., Wisthaler, A., and Fuentes, J. D.: Satellite isoprene retrievals constrain emissions and atmospheric oxidation, Nature, 585, 225–233, https://doi.org/10.1038/s41586-020-2664-3, 2020.

Wells, K. C., Millet, D. B., Payne, V. H., Vigouroux, C., Aquino, C. A. B., De Mazière, M., De Gouw, J. A., Graus, M., Kurosu, T., Warneke, C., and Wisthaler, A.: Next-Generation Isoprene Measurements From Space: Detecting Daily Variability at High Resolution, JGR Atmospheres, 127, e2021JD036181, https://doi.org/10.1029/2021JD036181, 2022.

Werner, C., Meredith, L. K., Ladd, S. N., Ingrisch, J., Kübert, A., Van Haren, J., Bahn, M., Bailey, K., Bamberger, I., Beyer, M., Blomdahl, D., Byron, J., Daber, E., Deleeuw, J., Dippold, M. A., Fudyma, J., Gil-Loaiza, J., Honeker, L. K., Hu, J., Huang, J., Klüpfel, T., Krechmer, J., Kreuzwieser, J., Kühnhammer, K., Lehmann, M. M., Meeran, K., Misztal, P. K., Ng, W.-R., Pfannerstill, E., Pugliese, G., Purser, G., Roscioli, J., Shi, L., Tfaily, M., and Williams, J.: Ecosystem fluxes during drought and recovery in an experimental forest, Science, 374, 1514–1518, https://doi.org/10.1126/science.abj6789, 2021.

Wiedinmyer, C., Greenberg, J., Guenther, A., Hopkins, B., Baker, K., Geron, C., Palmer, P. I., Long, B. P., Turner, J. R., Pétron, G., Harley, P., Pierce, T. E., Lamb, B., Westberg, H., Baugh, W., Koerber, M., and Janssen, M.: Ozarks Isoprene Experiment (OZIE): Measurements and modeling of the "isoprene volcano," J. Geophys. Res., 110, 2005JD005800, https://doi.org/10.1029/2005JD005800, 2005.

Wiedinmyer, C., Tie, X., Guenther, A., Neilson, R., and Granier, C.: Future Changes in Biogenic Isoprene Emissions: How Might They Affect Regional and Global Atmospheric Chemistry?, Earth Interactions, 10, 1–19, https://doi.org/10.1175/EI174.1, 2006.

Worden, H. M., Bloom, A. A., Worden, J. R., Jiang, Z., Marais, E. A., Stavrakou, T., Gaubert, B., and Lacey, F.: New constraints on biogenic emissions using satellite-based estimates of carbon monoxide fluxes, Atmos. Chem. Phys., 19, 13569–13579, https://doi.org/10.5194/acp-19-13569-2019, 2019.

Yáñez-Serrano, A. M., Nölscher, A. C., Williams, J., Wolff, S., Alves, E., Martins, G. A., Bourtsoukidis, E., Brito, J., Jardine, K., Artaxo, P., and Kesselmeier, J.: Diel and seasonal changes of biogenic volatile organic compounds within and above an Amazonian rainforest, Atmos. Chem. Phys., 15, 3359–3378, https://doi.org/10.5194/acp-15-3359-2015, 2015.

https://doi.org/10.5194/egusphere-2025-778
Preprint. Discussion started: 26 February 2025
© Author(s) 2025. CC BY 4.0 License.

Yáñez-Serrano, A. M., Bourtsoukidis, E., Alves, E. G., Bauwens, M., Stavrakou, T., Llusià, J., Filella, I., Guenther, A., Williams, J., Artaxo, P., Sindelarova, K., Doubalova, J., Kesselmeier, J., and Peñuelas, J.: Amazonian biogenic volatile organic compounds under global change, Global Change Biology, 26, 4722–4751, https://doi.org/10.1111/gcb.15185, 2020.

Zeinali, N., Altarawneh, M., Li, D., Al-Nu'airat, J., and Dlugogorski, B. Z.: New Mechanistic Insights: Why Do Plants Produce Isoprene?, ACS Omega, 1, 220–225, https://doi.org/10.1021/acsomega.6b00025, 2016.